JOINT INSTITUTE FOR NUCLEAR RESEARCH

2010-18

S. N. Dmitriev, M. G. Itkis

# REPORT ON THE ACTIVITY OF THE FLEROV LABORATORY OF NUCLEAR REACTIONS IN 2003–2009

Report to the 107th Session
of the JINR Scientific Council
February 18–19, 2010

Dubna 2010

S. N. Dmitriev, M. G. Itkis

# REPORT ON THE ACTIVITY OF THE FLEROV LABORATORY OF NUCLEAR REACTIONS IN 2003–2009

Report to the 107th Session
of the JINR Scientific Council
February 18–19, 2010

Dubna 2010

In this report we present the most important results of researches within the topics:

- 03-5-1004-94/2009 – "Synthesis of new nuclei and study of the nuclear properties and heavy ion reaction mechanisms",
- 03-5-1014-96/2009 – "Development of FLNR cyclotrons .for producing intense beams of accelerated ions of stable and radioactive isotopes",
- 03-0-0002-2000/2009 – Development and construction of accelerator complex for producing radioactive ion beams"

for the period 2003 – 2009:

## SYNTHESIS OF NEW NUCLEI AND STUDY OF NUCLEAR PROPERTIES AND HEAVY-ION REACTION MECHANISMS

Leader: M.G. Itkis, scientific leader: Yu.Ts. Oganessian

### Synthesis of superheavy elements

In order to synthesize superheavy nuclei in the vicinity of the predicted region of the increased stability complete fusion reactions of neutron-rich isotopes of actinides (Act.), such as $^{244}$Pu, $^{243}$Am, $^{248}$Cm, $^{249}$Bk and $^{249}$Cf as targets and the doubly magic nucleus $^{48}$Ca as projectile have been chosen [1].

The expected half-lives of heavy nuclei produced in these reactions can vary in a wide range: from a few μs up to tens of hours and the expected cross sections are calculated to be of the order of picobarns. The experiments have been performed employing the Dubna Gas-Filled Recoil Separator (DGFRS) of the FLNR JINR- [2-11].

The $^{48}Ca^{+5}$ ions, produced by the 14 GHz ECR ion source, were accelerated by the U400 cyclotron. The typical beam intensity at the target was 1.0-1.2 pμA. The consumption of the $^{48}$Ca isotope, enriched to 68%, amounted to about 0.5 mg/h.

In the experiments on the synthesis of superheavy nuclei, targets of actinide oxides were used with thickness of ≈ 0.35 mg/cm$^2$ deposited on a 1.5-μm Ti foil. Enriched isotopes of $^{233,238}$U [4], $^{237}$Np [15], $^{242,244}$Pu [4-6], $^{243}$Am [7-11], $^{245,248}$Cm [6,10,12], $^{249}$Bk [see text] and $^{249}$Cf [13,14] were used as target material.

In the reactions studied in [1-15], altogether 92 decay chains were registered. All decay chains are characterized, in their majority, by sequential α-decays (from one to six), which are terminated by spontaneous fission. In few cases, spontaneous fission occurred after detecting the recoil nucleus. In the observed chains, there were altogether 253 nuclear decays

The decay properties of the 34 new nuclides, produced in experiments with $^{48}$Ca projectiles (with exception of $^{249}$Bk+$^{48}$Ca), are given in figure 1.

In those cases, where two decay modes (α, *SF*) were observed, an approximate branching ratio, governed by the statistical error has been estimated. The values of $T_\alpha$ expected for the measured $Q_\alpha$ (see below) are presented in the sixth column.

The identification of the atomic numbers of the nuclides was performed in several independent ways based on: the mechanism of fusion reactions, the decay properties of the nuclei in the decay sequences and the radiochemical identification of the atomic number of the nuclides.

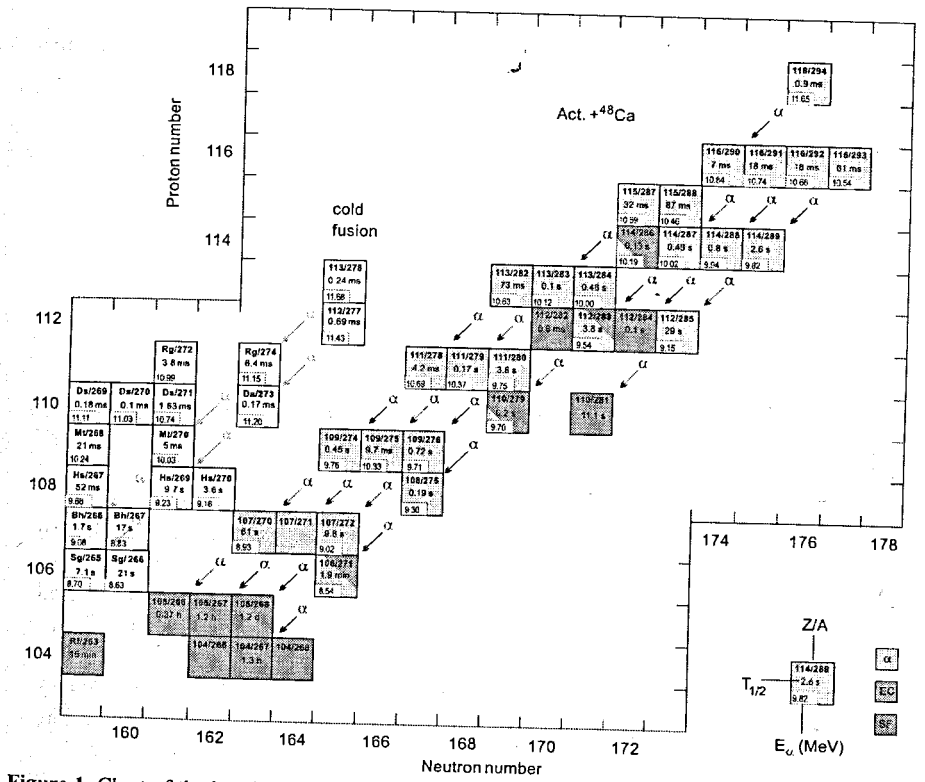


**Figure 1.** Chart of the heaviest nuclides with $Z \geq 104$ and $N \geq 159$. For the nuclei synthesized in cold fusion reactions the values of $T_{1/2}$ and $E_\alpha$ are taken from the compilation of ref. [16].

As a whole, the measured values of $Q_\alpha$(exp) are in agreement with theory, because the model calculations do not claim to be more precise in determining $Q_\alpha$(th) than 0.4-0.6 MeV.

The partial *SF* half-lives of nuclei with $N \geq 163$, produced in fusion reactions with $^{48}$Ca, together with the half-lives of *SF*-nuclides with $N \leq 160$, are shown in figure 2*a*.

The systematics of the total kinetic energies of spontaneous fission fragments from all known even-even isotopes with $Z \geq 96$ is shown in figure 2*b*. Two groups can be distinguished and are marked with dashed lines. They correspond to the



mass-asymmetric and mass-symmetric fission modes. These are characterized by a different dependence of *TKE* on $Z^2/A^{1/3}$ [17].

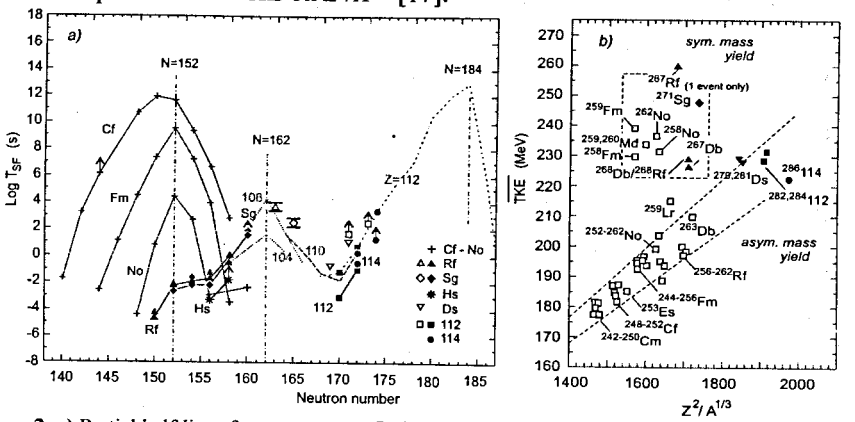


**Figure 2. a)** Partial half-lives for spontaneous fission $T_{SF}$ vs. $N$ for nuclei with even atomic numbers $Z$ = 98-114. Solid symbols and crosses denote even-even nuclei, whereas open symbols – even-odd nuclei. Black are the experimental data, red – the calculated $T_{SF}$ values. Solid black lines are drawn through the experimental points $T_{SF}$(exp) of even-even nuclei, the red lines – through $T_{SF}$(th), obtained in calculations [18] for even-even isotopes with $Z$ = 104-112. **b)** Systematics of mean total kinetic energies of fission fragments <*TKE*> vs. the parameter $Z^2/A^{1/3}$. The open squares are experimental data for the isotopes with $Z$ = 96-104 [17], the black symbols – the data for *SF*-isotopes with $Z \geq 104$, observed in Act. + $^{48}$Ca reactions. The dashed lines separate the zones of mass asymmetric and mass symmetric fission modes.

In experiments with accelerated ions of $^{48}$Ca isotopes of superheavy elements with Z = 111 ÷ 116 and 118 have been synthesized in 2001 - 2006. Synthesis of the element with Z=117 was necessary not so much to fill up the gap between 116 and 118, but to a great extent for producing data concerning properties of more than 15 new superheavy isotopes which are expected to be observed in decay chains.

The most perspective for synthesis of element Z=117 is the reaction $^{48}$Ca + $^{249}$Bk. However, preparation of a target from the unique $^{249}$Bk isotope is connected with significant problems: owing to short life time ($T_{1/2} \doteq 320$ d.). This isotope cannot be produced and accumulated in advance, and after production should be "used" immediately.

Since July 2009 till now the experiment is under way aimed at the synthesis of the new element 117 in the complete-fusion reaction $^{249}$Bk+$^{48}$Ca. The experiment is performed employing the Gas-Filled Recoil Separator of the FLNR JINR in collaboration with the laboratories of Oak Ridge (ORNL), Livermore (LLNL) and Vanderbilt University (USA). The target material was produced in Oak Ridge and the target itself was manufactured in RIAR Dimitrovgrad (Russia).

The target thickness was 0.31 mg/cm$^2$. In the first experimental run the energy of the accelerated $^{48}$Ca ions delivered by the U-400 cyclotron corresponded to the calculated maximum of the production of the isotopes $^{293}$117 and $^{294}$117, the products of evaporation of 3 and 4 neutrons from the compound nucleus $^{297}$117, that corresponded to the excitation energy of the compound nucleus of about 39 MeV. The total accumulated beam dose of $^{48}$Ca was $2.4\times10^{19}$. Altogether 5 decay chains

consisting from 3 α-decays and terminated by spontaneous fission were observed at this excitation energy.

In the end of October, 2009 another experiment has been started at a lower $^{48}$Ca energy that corresponds to the excitation of $^{297}$117 of about 35 MeV. At the end of December 2009 the collected beam dose amounted $1.2\times10^{19}$. The decay chain consisting from 6 α-decays and terminated by spontaneous was observed at this excitation energy. The data analysis is in progress.

Relative to the 30-year old history of investigations on heavy nuclei in cold fusion reactions that have led to the discovery of 6 new elements, the results obtained in Act. + $^{48}$Ca reactions are the next step in the synthesis and studies of the properties of new, heavier elements. The neutron-rich and rather long-lived nuclides, produced with cross sections of few picobarns in Act. + $^{48}$Ca reactions, are unique objects whose nuclear structure, decay modes, spontaneous fission, atomic and chemical properties have to be studied.

## Chemistry of superheavy elements

The investigation of chemical properties of the new nuclides is of separate interest in connection with the study of the structure of superheavy atoms and of the chemical behavior of the heavy and superheavy elements. At the same time, one of the direct methods of atomic-number identification is based on classical chemical methods.

Such a possibility is now opened for a series of neutron-rich relatively long-lived nuclei synthesized in Act. + $^{48}$Ca reactions. Some of them have half-lives ranging from several seconds to ~1 d, times – reachable by radiochemical methods (fig.3). Below the results on the chemical isolation of two nuclides: $^{268}$Db ($T_{SF}\approx$ 1.2 d) and $^{283}$112 ($T_{\alpha}\approx$ 4 s) are presented.

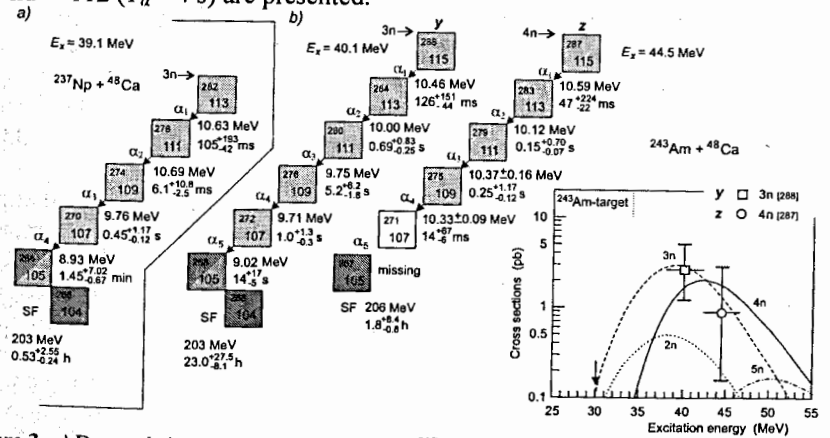


**Figure 3.** *a)* Decay chains, observed in the reaction $^{237}$Np + $^{48}$Ca [15]. *b)* Correlated decay chains *y* and *z*, obtained in the reaction $^{243}$Am + $^{48}$Ca at two excitation energies of the compound nucleus [7,8]. On the right-hand side of the chains the calculated excitation functions of the *xn*-evaporation channels of the $^{243}$Am + $^{48}$Ca reaction are shown. The points with error bars are the experimental cross sections.



*Chemical separation of $^{268}$Db*

As shown above, the longer-lived *R*-$\alpha_1$-...-$\alpha_5$-*SF* decay chains terminated by a *SF*-nuclide ($T_{SF}$ = $16^{+19}_{-6}$ h) were associated with the decay of the odd-odd isotope $^{288}$115, produced in the 3*n*-evaporation channel of the $^{243}$Am + $^{48}$Ca reaction.

Since all consecutive α-decays and *SF* are strongly correlated and the order of occurrence of the nuclei in the decay chains is determined, *the identification of the atomic number of any nucleus in this chain* would independently prove the synthesis of the previously unknown elements 115 and 113.

According to the atomic configuration in the ground state, Db should belong to the 5$^{th}$ group of the Periodic Table, as a heavier homologue of Nb and Ta. For the purpose of chemical identification, Db can be separated, along with the members of chemical group 5, from the other elements.

The rotating target consisted of the enriched isotope $^{243}$Am in the oxide form. The target material was deposited onto 1.5-μm Ti foils to a thickness of about 1.2 mg/cm$^2$ of $^{243}$Am. It is noteworthy that in comparison with the experiment at DGFRS, the target thickness is 3 times bigger. On leaving the target, the recoiling products stopped in a copper block positioned downstream from the target. The collection efficiency of EVRs was close to 100%. After the end of the irradiation, a thin Cu was cut from the catcher surface using a micro-lathe and dissolved in concentrated $HNO_3$. All procedures starting from the end of irradiation until the beginning of detector measurements took 2 to 3 hours.

For the registration of α-particles and spontaneous fission fragments, the sample was placed between two 6-cm$^2$ silicon detectors. Four chambers with detectors were located inside a neutron detector for the registration of spontaneous fission neutrons.

In June 2004 a total of eight similar irradiations of duration between 20 and 45 hours each were performed. A total $^{48}$Ca ions beam dose of $3.4\cdot10^{18}$ was collected in this experiment.

In eight irradiations of the $^{243}$Am target with $^{48}$Ca ions, 15 spontaneous fission events were detected. The measurements were carried out for 957 hours. All *SF* events appeared in a 174-hour interval following the start of the measurements. No events were detected in the next 783 hours. Run conditions and results of measurements are given in [9,10]. The spectrum of high energetic events measured with sample No 4 is presented in fig. 4.

In the second experiment, a more sophisticated method was used. It made it possible to completely separate the elements of group 5 (Nb, Ta, Db) from the elements of group 4 (Zr, Hf, Rf), as well as to separate the homologues Nb and Ta. In this experiment five events, corresponding to the decay of $^{268}$Db, were observed, all of them in the group 5 fraction, in agreement with its relationship to the closest homologue – Ta [11].

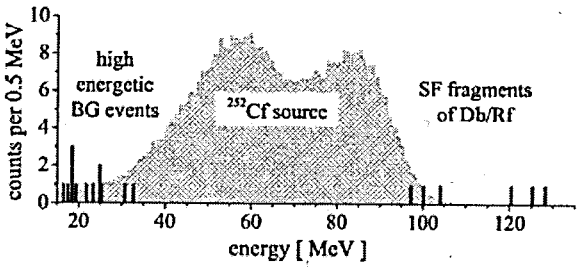


**Figure 4.** SF-spectra of sample no. 4 measured in $4\pi$-counting geometry: originally coincident SF-events (red) [9]; high energetic events measured in this work during 3600 h (blue); $^{252}$Cf calibration spectrum measured in $2\pi$ geometry (cyan, scaled 1:100).

Over the course of the two chemistry experiments, 20 decays of a *SF* nuclide were observed with $T_{1/2}$=28 $^{+11}_{-4}$ h and a total deposited energy $E_{tot} \approx$ 230 MeV [9-11]. The production cross section for *SF* nuclei, produced in the $^{243}$Am + $^{48}$Ca reaction, was 4.2 $^{+1.6}_{-1.2}$ pb. These results agree with the original element-115 synthesis experiment with DGFRS, where the same *SF* activity was first observed as the terminating isotope, following the five consecutive α-decays from the $^{288}$115 parent nucleus.

Thus, the data from the chemistry experiment give independent identification of the atomic number of all nuclei in the correlated decay sequence: $Z$ = 115 - α → 113 - α → 111 - α → 109 - α → 107 - α → **105** (*SF*). Moreover, it gives evidence of the synthesis of two new elements 115 and 113 in the reaction $^{243}$Am + $^{48}$Ca.

*Chemistry of element 112*

As is seen from the properties of nuclei in the observed decay chains (fig. 1), the most suitable for chemical studies are the odd isotopes of element 112: $^{283}$112 ($T_{1/2}$ ≈ 4 s) and $^{285}$112 ($T_{1/2}$ ≈ 30 s), undergoing α-*SF* decay.

According to the atomic configuration in the ground state, element 112 should belong to the 12$^{th}$ group of the Periodic Table as a heavier homologue of Hg, Cd and Zn. As it has been shown in the experiments [19], the Hg atoms in neutral gaseous atmosphere (e.g., in He or Ar at atmospheric pressure) can be transported together with the buffer gas to a significant distance (~30 m) with a velocity of up to 5 m/s. Therefore, investigation of gas adsorption properties of element 112 on metal surfaces has been suggested.

To what extent element 112 is a homologue of Hg depends on the so-called "relativistic effect" in the electronic structure of the superheavy atom. According to some relativistic calculations, the chemical behavior of element 112 will somewhat differ from that of its light homologue. The reaction $^{242}$Pu($^{48}$Ca,3*n*)$^{287}$114-α → $^{283}$112 [4] was used to produce the isotope $^{283}$112 [20,21]. The energy of the $^{48}$Ca beam corresponded to the maximum yield of the isotope $^{287}$114 ($T_{1/2}$ ≈ 0.5 s) – the



product of the 3*n*-evaporation channel of the fusion reaction $^{242}$Pu + $^{48}$Ca (see figure 5*b*, sequence ***o***).

The chemical setup applied in the experiments was based on the thermochromatographic in situ volatilization and online detection technique (IVO) in combination with the cryo-online detector COLD [22].

To the $^{242}$Pu-target (99.93%) about 15 μg/cm$^2$ of $^{nat}$Nd was added; this allowed to simultaneously produce the neutron-deficient short-lived α-radioactive $^{185}$Hg isotope having a half-life of 49 s, which served to monitor the production and separation processes.

The recoil nuclei leaving the $^{242}$Pu-target stopped in a high-purity gaseous medium: He(70%)+Ar(30%).

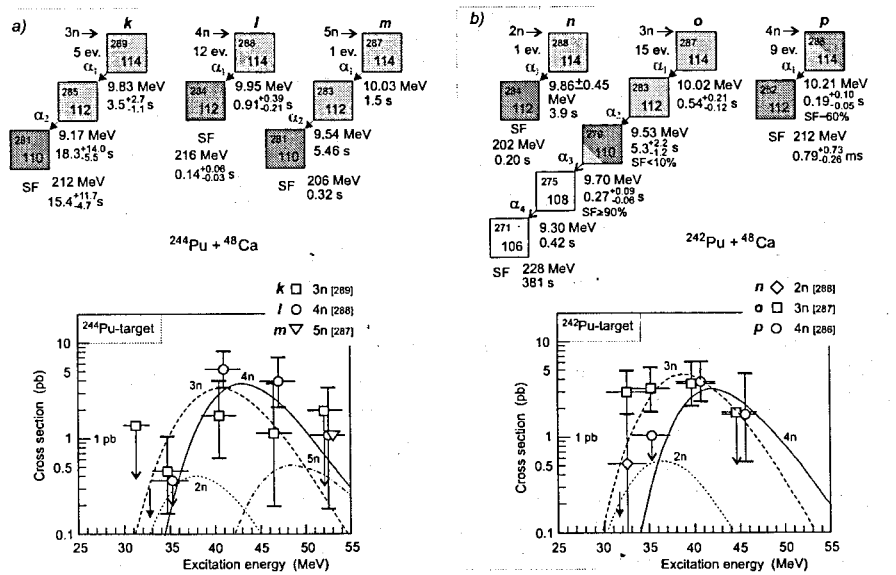


**Figure 5.** a) *Upper panel*: sequences of correlated decays in the $^{244}$Pu + $^{48}$Ca reaction. The one-type chains are shown as one decay-sequence and are denoted by ***k***, ***l***, and ***m***. b) As *a*) for the $^{242}$Pu + $^{48}$Ca reaction (sequences ***n***, ***o***, and ***p***).*Lower panel*: production cross sections of nuclei having the shown decays (denoted by letters) at different excitation energies of the compound nucleus.

The recoiling nuclei, which stopped in the He/Ar medium, were transported to the detectors by means of a 8m-capillary tube (fig. 6). The total transport time from the reaction chamber to the detectors was 3.6 s. This time is long enough for the decay $^{287}$114(0.5s)-α → $^{283}$112. Also, only about 50% of the daughter nuclides $^{283}$112 reached the detector chamber.

The setup COLD [22] consists of 32 pairs PIPS (passivated ion-implanted planar silicon) detectors, about 1 cm$^2$ each, placed one opposite the other with a 1.5 mm gap in between, through which the He/Ar gas flows. One of the detectors of each pair was covered with a 30-50-nm gold layer. The temperature gradient along the whole length of the detectors spanned a range from -30°C to -184°C in the first

experiment and from +30°C to -180°C in the second one. The energy resolution for decay α-particles amounted to 120 keV. The *SF* fission fragment energy was calibrated using a thin $^{248}$Cm source.

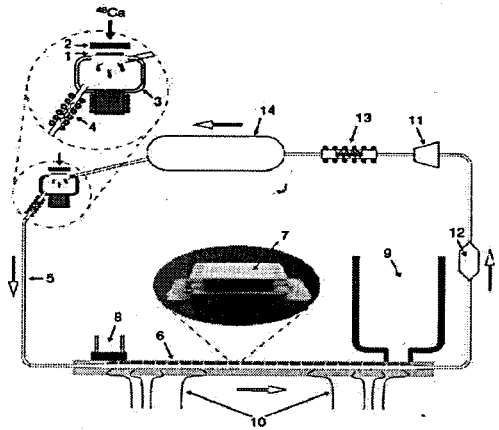

**Figure. 6.** $^{242}$Pu target (1), Ti vacuum window (2), stopping volume (3). quartz wool filter (4), Teflon capillary (5), thermochromatographic detector array "COLD" (6), 32 pairs of ion-implanted planar silicon detectors (7), thermostat (8), liquid nitrogen cryostat (9), thermometers (10), metal bellows pump (11), drying unit (12), getter oven (13), buffer volume (14). The white arrows indicate the direction of the gas flow [20].

In the control experiments, only α-particles from the decay of $^{181\text{-}188}$Hg (the fusion $^{nat}$Nd + $^{48}$Ca reaction), $^{211}$At and $^{219,220}$Rn were observed. As it was expected, only nuclei with high volatility were transported to the detectors. It was shown that all Hg atoms are registered by the first detectors with the Au coating. On the contrary, the decay of the chemically neutral Rn atoms is observed in the region of the last detectors, which are at the lowest temperatures.

The obtained thermochromatographic deposition patterns for $^{185}$Hg, $^{219}$Rn, and $^{283}$112 at varied experimental conditions are depicted in fig. 7 and represent a characteristic example for the gas chromatographic behavior of single atoms.

In the first experiment in 2006 [20] (fig. 7a) a spontaneous, diffusion-controlled deposition of $^{185}$Hg was observed in the first eleven detectors. $^{219}$Rn deposited almost entirely on the last nine detectors. Under these conditions one decay chain (fig .8, chain 1) related to $^{283}$112 was observed on the second detector (-28 °C) together with $^{185}$Hg, thus clearly distinct from $^{219}$Rn.

In the second part of the experiment in 2006 (fig. 7b) $^{185}$Hg revealed a shorter deposition pattern up to detector eight. Only 70% of the $^{219}$Rn was deposited in the last six detectors. A decay chain (chain 2) attributed to $^{283}$112 was observed on detector 7 (-5 °C).

In the 2007 experiment [21] (fig. 7c) the gas flow rate was increased to 1500 mL/min. The $^{185}$Hg deposition region broadened drastically to 14 detectors. Only about 30% of the $^{219}$Rn deposited on the last four detectors. The faster carrier gas transported also the three observed atoms of $^{283}$112 further down to detectors of



lower temperature. Two of the atoms (chain 3 and 5) deposited on the detectors 11 (-21 °C) and 14 (-39 °C). The third atom (chain 4) was transported even more downstream and deposited on detector 26 (-124 °C).

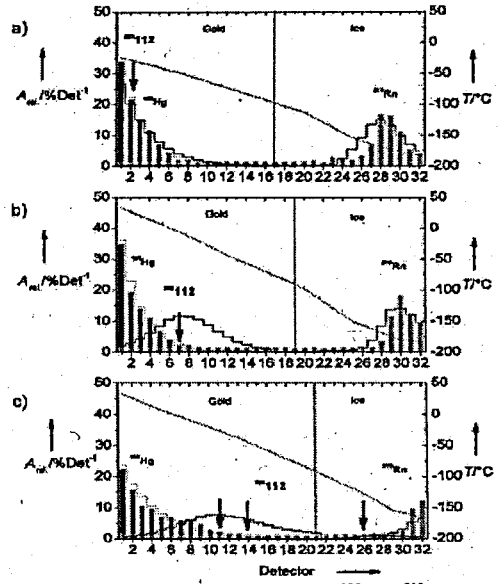


**Figure 7.** Thermochromatographic deposition patterns of $^{185}$Hg, $^{219}$Rn, and $^{283}$112 in the COLD, dependent on experimental parameters. The measured relative activity per detector (Arel., left-hand axis) of $^{185}$Hg (dark gray bars, MCS: gray dashed line) and $^{219}$Rn (gray bars, MCS: gray solid line) is shown. The positions of the detected $^{283}$112 atoms are indicated (black arrows, MCS: black solid line). The temperature gradient is shown (black dashed line, right-hand axis).

From results of permanent dew point measurements in the carrier gas, it has to be assumed that a thin ice layer was covering the detector surfaces held below -95 °C (fig. 7a–c, vertical lines). Therefore, we conclude that four events (chains 1–4) are attributed to atoms of element 112 deposited on the gold surface, and one event (chain 5) represents an atom of element 112 deposited on ice.

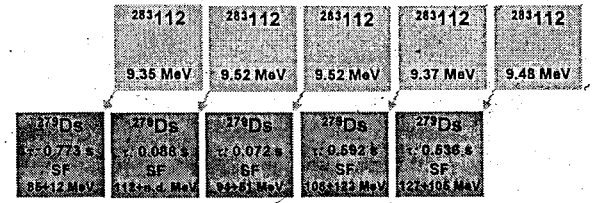


**Figure 8.** Detected α–SF decay chains assigned to the isotope $^{283}$112; n.d.=not determined.

The statistical analysis of the deposition behavior of $^{283}$112 (fig. 7, black arrows) revealed a standard adsorption enthalpy of element 112 on gold surfaces of $-\Delta H_{ads}^{Au}(112)=52^{+4}_{-3}$ kJ·mol$^{-1}$ (68%confidence interval). The observed enhanced adsorption enthalpy of element 112 on gold compared to the predicted adsorption

enthalpy indicates a metallic-bond character involved in the adsorption interaction between element 112 and gold.

By applying the estimated values for the sublimation entropy $\Delta S_{subl}$=106.5±2.0 J·mol$^{-1}$K, element 112 can be presumed to have a boiling point of 357±110 K. These values indicate that element 112 is considerably more volatile compared to its lighter homologues Zn, Cd, and Hg, thus manifesting the preserved trend of increasing stabilization of the elemental atomic state owing to relativistic effects in the electronic structure along Group 12 of the periodic table up to element 112.

The production cross section of $^{283}$112 in the reaction $^{242}$Pu($^{48}$Ca,3*n*)$^{287}$114-α → $^{283}$112 is estimated from the chemical experiments as 2-4 pb (from the DGFRS measurements $\sigma_{3n} = 3.6^{+3.4}_{-1.7}$ pb [4]).

The results of the given experiment in an independent way confirm the identification of the atomic numbers of the nuclides in the even-*Z* nuclear decay chain $^{291}$116 → $^{287}$114 → $^{283}$**112** → $^{279}$110 → $^{275}$108 → $^{271}$106 → $^{267}$104.

*Gas phase chemistry of element 114 (preliminary results [23])*

In the same experimental conditions, it is possible to investigate "long-lived" isotopes of the element 114 (see fig. 1).

The formation of $^{286-289}$114 (fig. 5) was observed in the nuclear fusion reactions of $^{48}$Ca on $^{242,244}$Pu [4-6]. Due to observed longer half-lives of up to several seconds chemical investigations of element 114 appeared to be feasible.

The systematic order of the periodic table places element 114 into group 14 together with carbon, silicon, germanium, tin, and lead. The enhancement of metallic character with increasing atomic number Z is an obvious trend observed along the main groups 13-17 of the periodic table. Thus, a metallic character can be expected for element 114. However, relativistic calculations of the electronic structures of SHE suggest contraction of the spherical s- and $p_{1/2}$- electron orbitals, increasing the chemical stability of the elemental atomic state for element 114. Therefore, a high volatility and a chemical inertness were postulated for this element.

In experiment [21], aimed at the investigation of chemical properties of the element 112 rather unexpectedly, one decay chain was observed, which was unambiguously attributed to the decay of $^{287}$114. Even more surprising was the observation of this decay chain on detector 19, held at a temperature of -88 °C

In a special thermochromatography experiment devoted to the element 114 a $^{244}PuO_2$ target (1.4 mg·cm$^{-2}$) deposited on a Ti backing (0.7 mg·cm$^{-2}$) was irradiated for 17 days with a beam dose of 4.5·10$^{18}$ $^{48}$Ca [23]. The target setup and beam properties were the same as in [21].

The half-lives of $^{288}$114 and $^{289}$114 are determined as 0.8 s and 2.6 s, respectively, suggesting a higher transport yield compared to $^{287}$114.

One decay chain, which is unambiguously attributed to the isotope $^{288}$114($T_{1/2}$=0.8 s, α), was observed on detector 18 held at -84 °C, fully confirming



the first observation [21]. Another interesting event, which was tentatively attributed to the in-flight decay of $^{288}$114, was measured on detector 3 (-4 °C). The correlated SF-decay of the genetically linked $^{284}$112 was observed three detectors downstream, on detector 6. The identification of the very short-lived genetically linked α-SF-decay chains of $^{288}$114 with correlation times of less than 0.5 s was unambiguous.

In the next experiment the chemical separation device COLD was installed behind the Dubna Gas-Filled Recoil Separator. Rotating targets of $^{244}PuO_2$ (0.4 mg·cm$^{-2}$) deposited on a Ti backing foil (0.7 mg·cm$^{-2}$) were irradiated with a beam dose of 9.7·10$^{18}$ $^{48}$Ca during 35 days.

The excellent background suppression using such physical preseparation is accompanied unfortunately by a factor of about 2-3 loss in overall efficiency.

At a deposition temperature of -93 °C on detector 19 one decay chain was observed that was attributed unambiguously to the decay of $^{285}$112 and its daughter $^{281}$Ds, which are the descendants of $^{289}$114.

The resulting adsorption enthalpy of element 114 on Au is $-\Delta H^{Au}_{ads}$(E114) = $35^{+4}_{-3}$ kJ/mol (68% credibility interval).

The comparison between theoretical predictions and our experimental result suggests the formation of a noble-gas like weak physisorption bond between atomic 114 and a gold surface. The experimental result points therefore to a substantially increased stability of the atomic state of element 114 that might be explained by a relativistic shell closure in the valence electronic structure.

The luminosity of the chemical experiment can be improved several times by means of increasing the beam intensity (rotating target) and the velocity of transporting the recoiling ions to the detectors. All this demonstrates the perspectives provided by Act. + $^{48}$Ca for the study of the chemical properties of superheavy elements.

**Investigation of reactions perspective for the synthesis of SHE**

The heaviest isotope that can be used for the synthesis of SHE as a target is $^{249}$Cf. Fusion of $^{249}$Cf with $^{48}$Ca ions leads to the nuclei of element 118 synthesized in 2005. Further investigations in the domain of superheavy elements call for using beams of ions heavier than $^{48}$Ca. Other than HI + Act. reactions, e.g. "symmetric" combinations Target + Projectile are also of great interest for the production of SHE.

*Study of the complete fusion reaction $^{226}Ra$ + $^{48}Ca$ (preliminary results)*

With a heavier projectile the production cross section of the resulting nuclei could considerably decrease. In order to determine this possible reduction we started the experiments on measuring the cross sections of the complete fusion

reactions $^{226}$Ra+$^{48}$Ca and $^{226}$Ra+$^{50}$Ti with evaporation of 3-5 neutrons. Comparing the cross sections of the complete fusion reactions with ions of $^{48}$Ca and $^{50}$Ti one can estimate more accurately the cross sections of the complete fusion of the nuclei of $^{243}$Am, $^{249}$Bk, $^{249}$Cf with $^{50}$Ti ions and thus to clear the prospects of the synthesis of new elements 117, 119 and 120.

The series of the experiments aimed at the study of the complete fusion of $^{226}$Ra and $^{48}$Ca was accomplished at the DGFRS. The energy of $^{48}$Ca corresponded to the excitation energy of the compound nuclei in the range 34< E*< 48 MeV.

According to the calculations these energies correspond to the maximum yield of products of the complete fusion reaction $^{226}$Ra+$^{48}$Ca with evaporation of four and three neutrons, resulting in the formation of the isotopes $^{270}$Hs and $^{271}$Hs.

Earlier these isotopes were observed in the reaction $^{248}$Cm+$^{26}$Mg that leads to the same compound nucleus $^{274}$Hs. In those experiments the energy of the α-particles of $^{270}$Hs was measured, $E_\alpha$=8.88±0.05 MeV. The half-life could not be determined, as the time of the formation of the nuclei was not registered. For the daughter nucleus $^{266}$Sg spontaneous fission with a half-life of $0.36^{+0.25}_{-0.10}$ s was observed. The cross section of this reaction makes about 3 pb.

The measured α-particle energy is 9.03±0.09 MeV and the half-life of this nucleus is $9.7^{+9.0}_{-3.1}$ s. For the spontaneously fissioning isotope $^{266}$Sg the half-life was measured to be $0.21^{+0.20}_{-0.07}$ s.

The decay chains of six nuclei of $^{270}$Hs observed in these experiments are given in fig. 9.

The cross section of the reaction $^{226}$Ra($^{48}$Ca,4$n$)$^{270}$Hs at the $^{48}$Ca energy of 233 MeV is $9.0^{+11.5}_{-4.9}$ pb. At the energies of 229 MeV and 240 MeV the nuclei of element 108 were not observed.

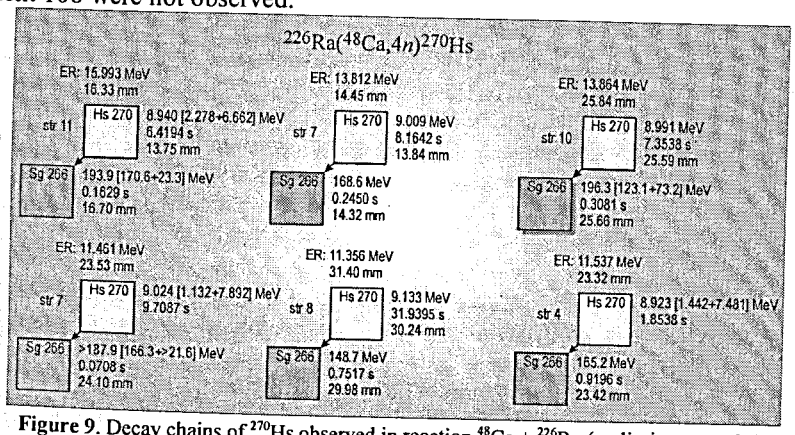


**Figure 9.** Decay chains of $^{270}$Hs observed in reaction $^{48}$Ca + $^{226}$Ra (preliminary results).

The data are now under analysis



*Attempt to produce element 120 in the $^{244}$Pu + $^{58}$Fe reaction*

Three reactions, $^{238}$U + $^{64}$Ni, $^{244}$Pu + $^{58}$Fe, or $^{248}$Cm + $^{54}$Cr, can be used for synthesis of isotopes of element 120, all leading to the same compound nucleus, $^{302}$120 ($N$ = 182).

In the reaction $^{244}$Pu + $^{58}$Fe, the excitation energy at the Coulomb barrier ($B_{Bass}$ = 310.5 MeV) is $E^*$ = 29.4 MeV the maximum yield of the evaporation residues is expected for the 3$n$- and 4$n$-evaporation channels that result in the formation of the isotopes $^{299}$120 and $^{298}$120.

According to theoretical predictions the even-odd nuclide $^{299}$120 should undergo α –decay with a decay energy in the range of $Q_\alpha$ = 11.5–13.2 MeV and a half-life of $T_\alpha$ ~ 1 μs –10 ms. The half-life of the even-even nucleus $^{298}$120 should also considerably exceed 1 μs.

Irradiation of the $^{244}$Pu target by $^{58}$Fe projectiles was performed using DGFRS and the $^{58}$Fe accelerated by the U400 cyclotron [24]. The decay chains that could be assigned to the isotopes of element 120 or its daughter nuclei were not observed during an irradiation with a beam dose of $7.1\times10^{18}$ of the 330-MeV $^{58}$Fe projectiles expected for the 4$n$-evaporation channel. The sensitivity of the experiment corresponds to 0.4 pb for the detection of a single decay (1.1 pb is the upper cross-section limit). The low cross section together with that measured for the reaction $^{249}$Cf($^{48}$Ca,3$n$)$^{294}$118 in comparison with the corresponding values for $Z$=114 and 116 nuclei could indicate receding from the stability region at $Z$=114.

On the other hand, the difference in the cross sections of the reactions with $^{244}$Pu nuclei can be a consequence of a strong increase of the dynamic hindrance with the increase of the projectile charge and mass when changing from $^{48}$Ca to $^{58}$Fe projectiles.

*Experimental study of the $^{136}$Xe + $^{136}$Xe reaction.*

The experiment aimed at the study of the symmetric reaction $^{136}$Xe+$^{136}$Xe→$^{272}$Hs* was performed in June-July 2007. The beam of $^{136}$Xe$^{16+}$ with an intensity of about 2.5 eμA passed through a 4 μm Ti separating foil at the initial energy of 750 MeV. The target (99% $^{136}$Xe enrichment) was kept at normal pressure. The target thickness was $3\times10^{18}$ Xe atoms (2.5 mg/cm$^2$). The beam energy in the centre of the target chamber was 650 MeV. Nuclear reaction products were stopped in the chamber, through which the transport gas (70% He, 20% Ar and 10% $O_2$) passed with a velocity of 0.9 l/min.

The reaction products were transported with the carriert gas flowing through a 30 cm long quartz tube containing a quartz wool plug. The tube was heated to 650° C and served as a filter for aerosol particles and provided an extended surface for the oxidation reaction of Os and Hs into their tetraoxides. The oxides were transported through a 8 m long perfluoroalkoxy (PFA) tube to the detection system.

The detection system consisted of 8 pairs of silicon PIN-photodiodes 1×1 $cm^2$ in the active area. The distance between the opposite PIN diodes was 1.5 mm.

The detection system was kept at -50° C according to the deposition temperature of $HsO_4$. The model experiment with the reaction $^{20}Ne+^{156}Dy \rightarrow ^{176}Os^*$ was performed to test the gas transport equipment and the detection system, to estimate the transport time of recoil nuclei and select appropriate parameters for the main experiment. During the model experiment the gas transport time of 3 s was measured using $^{169}Os$. Over a period of four weeks $3.6\times10^{17}$ ions were delivered to the target. Observation of one decay corresponds to the cross section of ~ 3 pb at given experimental conditions. Neither spontaneous fission nor alpha decay with energy of higher than 7 MeV were observed [25].

**Reactions induced by stable and radioactive ion beams of light elements**

Research with radioactive ion beams (RIBs) is an important trend in nuclear physics. The investigation of nuclei far from the β-stability valley and even beyond the nuclear stability lines (the driplines) is important for understanding the properties of nuclear matter at extreme conditions. It is necessary for the further development of nuclear theory and indispensable for nuclear astrophysics.

Progress in the production of very short- lived nuclei and the development of radioactive nuclear beams have given this field the necessary tools for detailed studies of the most exotic nuclei. The availability of radioactive beams have already provided conspicuous results on halo structures, shell inversion or new magic numbers and exotic decay modes showing up at the nuclear stability borders.

Not only well established approaches to RIB research have been used. A novel approach to the investigation of resonant states of nuclei close to and beyond the neutron dripline has been proposed, developed, and practically applied. It succeeded to show that in the experiments performed with certain kinematic settings, correlations inherent to the reaction products become an extremely rich source of information.

A unique technical feature is the availability of tritium beams and cryogenic tritium targets in FLNR. At the moment it is the only place in the world where the availability of the tritium target and beam is combined with RIB research. The following main results have been obtained in 2003 - 2009:

- For the first time the spectra of the $^3H(^2H,p)^4H$ and $^3H(^3H,d)^4H$ reaction products arising from the population of the $^4H$ ground state (g.s.) resonance were disentangled from events coming from different reaction mechanisms and the parameters of the $^4H$ g.s. were reliably derived [26].
- A lower limit for the $^7H$ decay energy was established in [27].
- The $^5H$ energy spectrum was reliably established [28]. The observed very anisotropic correlation pattern allowed one to identify this structure as a mixture of the $3/2^+$ and $5/2^+$ states (fig. 10). Such a unique spin identification of the three-body system using information coming from the correlations is a



novel feature of this study. As a result the experimental methods for the analysis of the three-body decays of spin-aligned states were developed and applied [29].

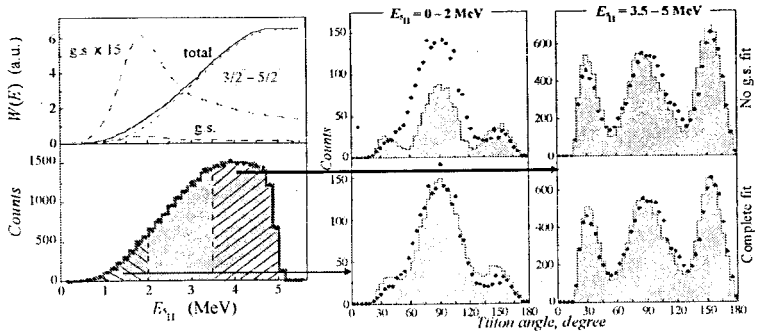


Figure 10. Missing mass spectrum of $^5H$ is quite featureless, showing only a broad structure above 2.5 MeV. However, correlation information allows:
a). Identify continuum above 2.5 MeV as a mixture of energy degenerate 3/2 and 5/2 states.
b). Explain the properties of continuum below 2.5 MeV as result of interference of 3/2 -5/2 doublet and 1/2 g.s.
c). To deduce properties of the $^5H$ g.s.: E ≈ 1.8 Mev, Γ= 1.3 MeV.

- The $^8He$, $^9He$, and $^{10}He$ spectra were revised in [30,31]. Before these works, the low-lying spectra of these nuclei have been considered as reliably established for more than a decade.

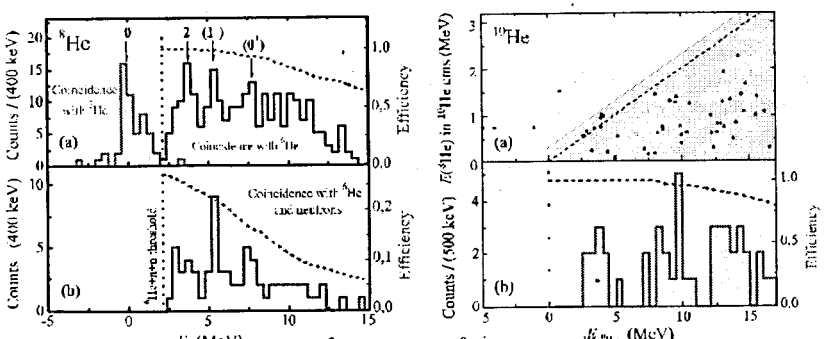


Figure 11. Missing mass spectra for $^8He$ (left) and $^{10}He$ (right).

- New data was obtained on the energy levels of $^{7\text{-}10}He$, $^{11}Li$, $^{13\text{-}14}Be$, as well as information on a series of neutron-rich nuclei (including $^{31}F$, $^{34}Ne$, $^{37}Na$, $^{43}Si$, etc.) in the region of the "island of inversion" [32].

- The total reaction cross sections in the interaction of $^{4,6}He$, $^{6,7}Li$, $^9Li$, $^7Be$, $^8B$ with Si-target nuclei were measured as a function of energy [33].

- In 2005 the first stage of the accelerator complex for radioactive beams DRIBs was put into operation. This facility provided a possibility to perform new, high level investigations of reactions induced by $^6He$ at energies in the vicinity of

the Coulomb barrier. The $^{6}$He-beam intensity at the physical target reached $10^{7}$ pps. The obtained results for the first time demonstrated that deep-sub-barrier fusion of nuclei with a neutron halo (such as $^{6}$He) is possible [34,35] (fig.12) and stimulated similar experimental and theoretical research of sub-barrier reactions with weakly bound nuclei in a number of scientific centers [36].

- Isomeric ratios for fusion and transfer reaction products, obtained in $^{6}$He-induced reactions on $^{197}$Au, were measured for the first time [37].

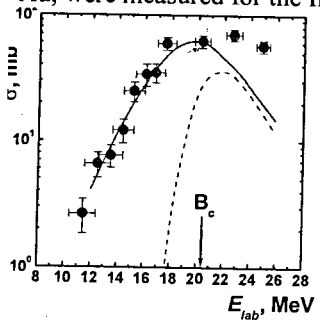


**Figure 12.** Excitation function measured for the $^{206}$Pb($^{6}$He, 2n)$^{210}$Po reaction [34,35,39]. The solid line denotes calculations using the two-step fusion model [34], whereas the dashed line – statistical model calculations, demonstrating the large excess of cross section below the Coulomb barrier $B_c$.

- Using $^{6}$He and $^{6}$Li beams an interesting result was obtained for neutron and deuteron transfer, respectively. In both cases a maximum cross section was observed at energies close to the Coulomb barrier of the reaction. The cross section for one-neutron transfer from $^{6}$He to the $^{197}$Au-target nucleus amounted to more than 1 barn [34,38,39].

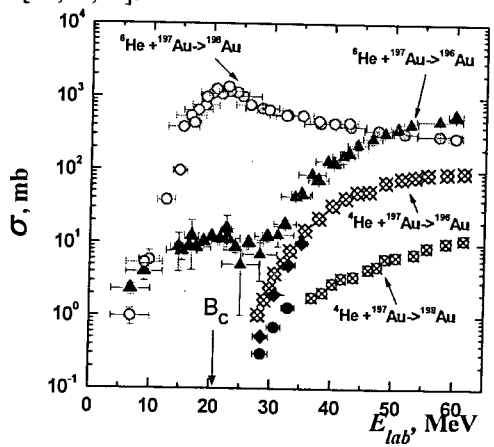


**Figure 13.** Excitation functions for the formation of the isotopes $^{198}$Au and $^{196}$Au in the interaction of $^{6}$He ions with $^{197}$Au [34,39]. For comparison, the excitation functions, obtained in $^{4}$He-induced reactions are shown.



- The momentum distributions of $^{4}$He from the breakup of $^{6}$He and $^{6}$Li nuclei were measured [40]. The small width of the momentum distribution in the case of the $^{6}$He beam confirmed the presence of a halo in this nucleus. The momentum distribution in the case of $^{6}$Li is wider than that for $^{6}$He, but narrower than those obtained for stable nuclei. This observation can be considered as demonstrating the fact that the $0^{+}$-excited state of $^{6}$Li has a halo-structure, which consists of a neutron+proton above the α-particle core and is characteristic of the increased radius of the nucleus in this state.

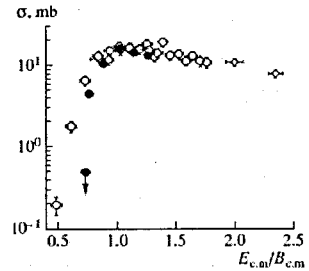


**Figure 14.** Excitation function for the production of the isotope $^{199}$Au (●) in transfer reactions when $^{6}$Li ions interact with a Pt target [38-40]. For comparison the excitation function for the fusion reaction d +$^{198}$Pt → $^{199}$Au (○) is shown.

## Fission and quasi-fission phenomena in heavy and superheavy nuclear systems

Study of the fusion-fission reactions at low incident energies gives us useful information on formation and survival probabilities of heavy nuclear system and allows one to choose optimal nuclear combinations for synthesis of superheavy elements.

The two-armed time-of-flight position sensitive spectrometer "CORSET" has been developed in 1994 at FLNR to study the collective motion of nuclear system formed in low-energy collisions of heavy ions [41]. The time-of-flight spectrometer CORSET, is presented schematically in fig. 15. It is capable of registering the angles, masses and energies of correlated fragments in a large solid angle ~ 0.3 sr.

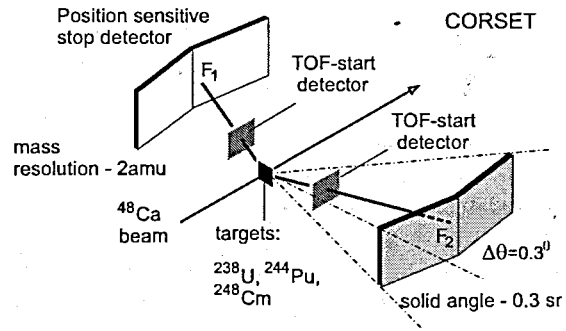


**Figure 15.** Layout of the CORSET setup for measuring masses and energies of fission fragments [42].

This setup in a combination with the multi-neutron detecting system DEMON allows one to study mass and energy distributions of reaction fragments in coincidence with neutron and gamma-ray emission.

For the first time, the experimental data for the three nuclear regions – pre-actinide, intermediate and transfermium – were obtained on the mass and energy distributions of reaction fragments, the multiplicities of pre- and post-neutron emission as well as on angular and energy neutron distributions in coincidence with fission fragments in a given mass and energy intervals.

In $^{204,208}$Pb($^{16}$O,f) and $^{208}$Pb($^{18}$O,f) reactions the multi-dimensional correlations (mass-energy-angle) of fission fragments in coincidence with gamma-rays were studied at incident energies close to the Coulomb barrier (excitation energies in the region of 16-40 MeV) [52]. Two fission modes (symmetric and asymmetric) were found at low excitation energies and agree well with predictions of macro-microscopic model.

Experimental study of fission probability, energy and mass distributions of fission fragments, post and pre-neutron emission was performed for the neutron-deficient thorium isotopes $^{220, 224, 226}$Th as well as for compound Ra-nuclei obtained in $^{204,208}$ Pb+C fusion reactions at near and sub-barrier incident energies [44].

Comparison of neutron multiplicity was performed for the $^{4}$He+$^{238}$U, $^{232}$Th, $^{208}$Pb ($E_{lab}$ = 60,75,97 and 220 MeV) and $^{16}$O + $^{238}$U, $^{232}$Th, $^{208}$Pb ($E_{lab}$=85 and 120 MeV) fusion reactions [45]. From analysis of the large block of experimental data the empirical description of pre-scission neutron emission was derived depending on excitation energy of compound nucleus. The following results were obtained:

(1) The ratio of symmetric and asymmetric fission was measured for $^{216,218,220}$Ra nuclei as a function of excitation energy. For the first time a manifestation of the "chance" structure in fission of these nuclei was observed.

(2) At the same excitation energy the relative probability for alpha-decay in competition with fission is one order of magnitude larger for radium isotopes as compared with thorium ones.

(3) Asymmetric fission of Ra nuclei is determined by formation of the two spherical shells, namely, (Z~50, N~82) in the heavy fragment and (Z~28, N~50) in the light one.

(4) Quite different mass distributions of fission fragments were found for $^{216}$Ra formed in the $^{12}$C + $^{204}$Pb and $^{48}$Ca + $^{168}$Er fusion reactions at the same excitation energy of 40 MeV [46]. Sharp increase of asymmetric fission mode in the $^{48}$Ca + $^{168}$Er fusion reaction is definitely connected with the quasi-fission fission process defined by the shell effects.

The analysis of mass-angular correlations in the reactions $^{40}$Ca+$^{154}$Sm and $^{48}$Ca+$^{144,154}$Sm showed that the mass-angular distributions obtained for the $^{48}$Ca+$^{154}$Sm support the QF nature of the asymmetric component [47]. Preferential forward-peaking of the light-mass fission-fragments ($A_L$ = 73–82) demonstrates that QF bypass the CN stage and occurs in time scales shorter than the rotational period for the $^{202}$Pb*.



This leads to a broken forward-backward symmetry of the angular distribution in the c.m. system for the asymmetric masses of fission fragments. In contrast to $^{48}$Ca+$^{154}$Sm, symmetric angular distributions for all masses of fission fragments are clearly observed in the $^{48}$Ca+$^{144}$Sm reaction. In the last case a CN nature of fission fragments is implied, i.e., one can state that the projectile-target system leading to $^{192}$Pb* lives so long that is enough for several rotations.

Thus in the $^{48}$Ca+$^{144}$Sm reaction, no evidence of QF was found at the same CN excitation energy and angular momentum as in the case of the reaction with $^{154}$Sm, where QF shows up. A small QF component has been also detected in the $^{40}$Ca+$^{154}$Sm reaction at energies close to the Coulomb barrier. So, the QF effect is manifested in the reactions with the deformed target nucleus $^{154}$Sm, which correspond to greater values of the entrance-channel mass-asymmetry than in the case of the $^{48}$Ca reaction with spherical $^{144}$Sm.

The compound nucleus, if formed in a fusion reaction, will prevailingly undergo fission from its initial (excited) state. The fission fragments of a compound nucleus have the characteristic mass and energy distributions, which distinguish them from fragments, formed in other exit channels: quasi-elastic scattering, deep-inelastic collisions, etc. The task is to separate the channel pertaining to the compound nucleus fission [47].

The total kinetic energies (TKE) of two correlated fragments, produced in the $^{208}$Pb + $^{48}$Ca reaction corresponding to full momentum transfer from the $^{48}$Ca ions to the composite system $^{256}$102 at $E_x$ = 18 MeV, are shown in fig. 16*a* as a function of the fragment mass ($A_F$). The observed fragments with mass around $A_P$ = 48 (projectile-like) and $A_T$ = 208 (target-like) are products of multi-nucleon transfer in quasi-elastic (QE) and deep-inelastic (DIC) collisions.

The region of mass and energy $A_F = A_{CN}/2 \pm 20$ and TKE = 200 ± 50 MeV, according to known data, covers about 60% of the fission fragments of $^{256}$No [48]. From the measurements at various energies, the fusion-fission cross section $\sigma_{FF}(E_x)$ was determined, which, in first approximation, for the reaction $^{208}$Pb + $^{48}$Ca can be taken as $\sigma_{CN}(E_x)$.

For the $^{206-208}$Pb + $^{48}$Ca reaction the cross sections of evaporation residues $\sigma_{xn}(E_x)$ were also measured earlier in the energy interval $E_x \approx$ 15-42 MeV for the *xn*-evaporation channels, when $x$ = 1-4. Thus, from the experiments with the $^{206,208}$Pb + $^{48}$Ca reaction, the complete pattern of fusion and survival of the compound No nuclei at different excitation energies could be unambiguously drawn.

In the followed experiments either the projectile mass was increased keeping $^{208}$Pb as a target (cold fusion) or the target mass was increased and the projectile used was $^{48}$Ca (hot fusion). The two-dimensional plot TKE vs. $A_F$, measured in the $^{208}$Pb + $^{58}$Fe reaction, is shown in fig. 16*b*. It is seen that when the projectile mass is increased from $^{48}$Ca to $^{58}$Fe, the picture changes drastically. The yields of the projectile-like and target-like products have increased significantly, whereas the yield of fragments corresponding to the region expected for the fission of the compound nucleus $^{266}$Hs has decreased by more than two orders of magnitude [52].

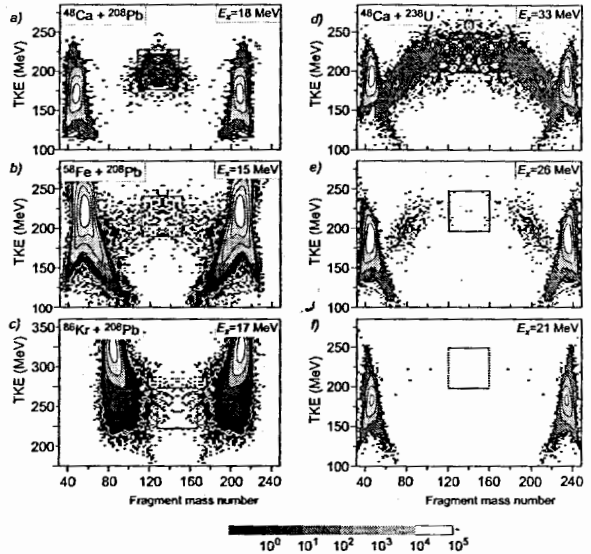


**Figure 16.** Two-dimensional spectra of $TKE(A_F)$ of correlated fragments from cold fusion reactions (indicated on the graphs *a* [48], *b* [49] and *c* [50]). The excitation energies of the nuclei $^{256}$102, $^{266}$108 and $^{294}$118 are shown on the graphs. The red line encircles the region of fragment mass $A_{CN}/2 \pm 20$ a.m.u. with summed kinetic energy $\langle TKE \rangle \pm 50$ MeV. The spectra, measured in the $^{238}$U + $^{48}$Ca reaction at different excitation energies of the $^{286}$112 nucleus are given in the graphs *d*, *e* and *f* [51].

Indeed, as it has been shown by different model calculations, here dynamical hindrances to the formation of the compound nucleus start to play an important role. Finally, in the reaction $^{208}$Pb + $^{86}$Kr (fig. 16*c*), in the mass region $A_{CN}/2$ only few events were registered; the upper limit for the formation of the compound nucleus with $Z = 118$ was estimated to be $\sigma_{CN} \leq 200$ nb.

The data for the $^{238}$U + $^{48}$Ca reaction at $E_x = 33$ MeV are presented in fig. 16*d*. In this reaction again, a large yield of projectile-like and target-like nuclei was observed, along with events in the region where fission fragments from the compound $^{292}$114 nucleus were expected. However, in contrast to the experiment with the $^{208}$Pb-target, the observed fragments are typical for strongly asymmetric fission (two egg-like distributions, symmetric relative to $A_{CN}/2$), and are situated outside the place where the compound nucleus fission fragments would come.

Obviously, this process – named "quasi-fission" (QF) – is not connected with the formation of the compound nucleus $^{286}$112, but its tails create a background in the symmetric mass region $A_F \approx A_{CN}/2$. The separation of these two types of fission is possible only by means of systematic measurements at various excitation energies, since the yields of the two types of fission vary at the different excitation energies (see fig. 16*d*, *e*, and *f*). The peak of the heavy fragments of quasi-fission is located close to $A_F \approx 208$ ($^{208}$Pb). Similar measurements were done also for many other reactions, with targets lighter or heavier than $^{238}$U [53,54].



The fission-fragment mass distribution, obtained in one of these reactions, $^{248}$Cm + $^{48}$Ca at $E_x = 33$ MeV, is presented in fig. 17*a*. The difference between the two types of fission is well seen: the main channel is QF, with mass ratio of the fragments $A_{F1}/A_{F2} \approx 2.35$, and the other one, of much less intensity (FF) – with $A_{F1}/A_{F2} \approx 1.24$. In the same figure, the known fission fragment mass distribution of $^{238}$U at $E_x \approx 33$ MeV is shown; its shape is quite similar to that of the *FF* mass spectrum from the reaction $^{248}$Cm + $^{48}$Ca.

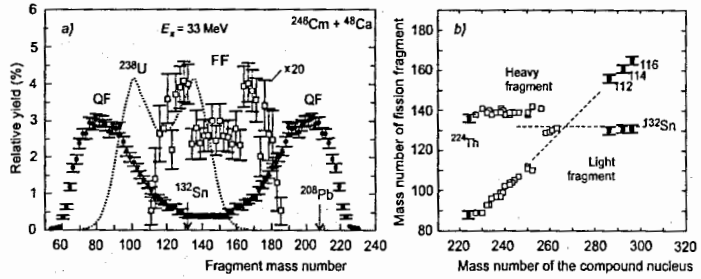


**Figure 17.** a) Mass distributions of quasi-fission fragments (black points) and fission in the symmetric mass region (open squares) in the $^{248}$Cm + $^{48}$Ca reaction at $E_x = 33$ MeV. The dashed line is the fission fragment mass distribution of $^{238}$U at $E_x = 30$ MeV. b) The most probable mass of the primary fission fragments as a function of the mass of the fissioning nucleus. The open squares denote low-energy fission of actinides, the black squares – fission of the excited nuclei with $Z = 112, 114, 116$.

The overlap of the mass of the heavy fragment from $^{238}$U and the mass of the light fragment from $^{296}$116 may be a sign that the fission in both cases is governed by the effect of the closed shells Z = 50, N = 82. The difference lies in that in the fission of $^{238}$U the shell effect is connected with the formation of the heavy fragment, while in the case of the heavy nucleus ($A = 296$) it manifests itself in the light fragment. As can be seen from fig. 17*b*, the mass distributions of the fragments from the *FF*-channel and the data, obtained for the actinides, show that the fission mode of all nuclei with Z = 90 to Z = 116 is very much the same. The mass and energy spectra of the fission fragments are characterized by a small change in the mass of one of the fragments (the Z = 50, N = 82 shell effect) and a large variation of the mass of the complementary fragment (depending on the mass of the fissioning nucleus).

Due to the same reasons, in the intermediate mass region A = 258–272, the mass-symmetric fission mode may prevail when the Z = 50, N = 82 shell effect works simultaneously on both fragments.

The results, obtained in the $^{238}$U, $^{244}$Pu and $^{248}$Cm + $^{48}$Ca experiments, can be shown in the form of collective motion of the heavy nuclear system over the potential energy surface. As illustrated in fig. 18*b* for the reaction $^{248}$Cm + $^{48}$Ca, at the contact point of the $^{248}$Cm and $^{48}$Ca nuclei, the potential energy of the nascent $^{296}$116 nucleus is *higher* than the energy of the compound nucleus. That is why in the reactions Act. + $^{48}$Ca, contrary to cold fusion (see for comparison fig. 18*a*), the hindrances to the formation of compact shapes must be considerably suppressed. This will in turn lead to an increase in the probability $P_{dyn}$.

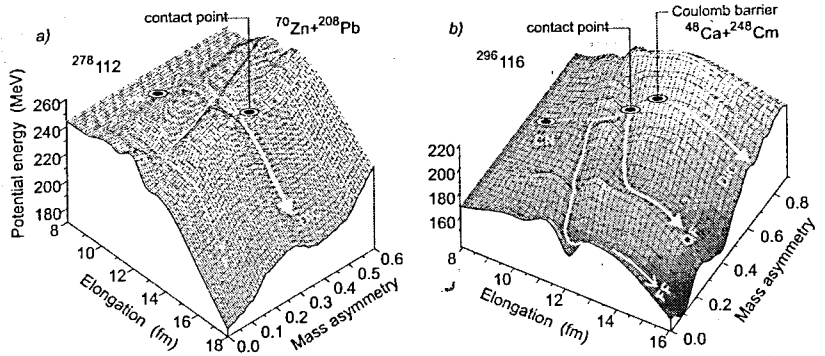


**Figure 18.** An illustration of the possible trajectories of collective motion of the nucleus on the potential energy surface [55] as a function of the deformation corresponding to the nuclear shape evolving from the touching point to the compact configuration of the compound nucleus: *a)* $^{278}112$ – in the cold fusion reaction $^{208}Pb + ^{70}Zn$, *b)* $^{296}116$ – in the reaction $^{248}Cm + ^{48}Ca$.

At the same time, at the early stage of the reaction, the system can, with high probability, enter the deeper valley of quasi-fission. Because of this loss, only a small part of the nuclei will reach compact forms close to the top of the compound nucleus fission barrier. The ratio of the yields of QF and FF displays the competition between these two processes. As is seen from fig. 18*b*, the cross section $\sigma_{CN}$ can be less than $\sigma_{FF}$, since the nucleus may enter the compound nucleus fission valley and demonstrate at the scission point the characteristics of fission without transition over the fission barrier (i.e., by-passing the stage of forming a compound nucleus, see fig. 18*b*).

Analysis of the obtained experimental data on the fusion and fission of the nuclei of $^{286}112$, $^{292}114$ and $^{296}116$ produced in the reactions $^{48}Ca+^{238}U$, $^{48}Ca+^{244}Pu$ and $^{48}Ca+^{248}Cm$ as well as experimental data on the survival probability of those nuclei in evaporation channels of 3 and 4 neutron emission allows one to derive the fission barriers of these superheavy nuclei which were found to be really quite high (resulting in relatively high stability of these nuclei). The lower limits obtained for the fission barrier heights of $^{283-286}112$, $^{288-292}114$ and $^{292-296}116$ nuclei are 5.5, 6.7 and 6.4 MeV respectively [56].

The energy-mass correlations were also measured for low-energy collisions of $^{58}Fe$ and $^{64}Ni$ with actinide targets $^{238}U$, $^{244}Pu$ и $^{248}Cm$ [57]. Direct comparison of the two fusion-fission reactions $^{64}Ni + ^{242}Pu \rightarrow ^{306}122$ and $^{58}Fe+^{248}Cm \rightarrow ^{306}122$ leading to the same compound nucleus demonstrates that in the first case the QF process is much higher than in the second one. This means that the iron beam is more favorable (as compared to Ni beam) for future experiments on synthesis of superheavy elements with Z>=120.

A search for three-cluster collinear decay of heavy nuclei was performed with the mini-FOBOS spectrometer and two-armed spectrometer on a base of micro-channel and PIN detectors [58].



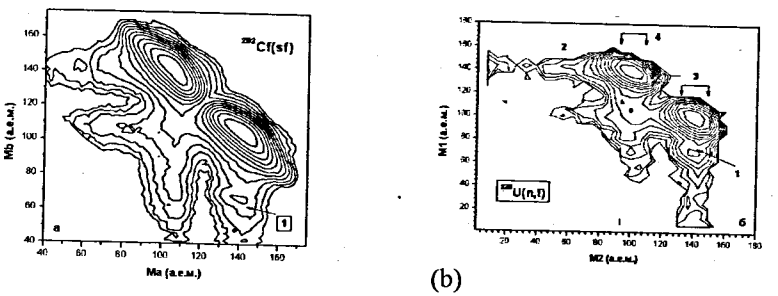


(a) (b)

**Figure 19.** Mass-mass distribution of fission fragments in the $^{252}Cf$ (sf) (a) и $^{235}U$ ($n_{th}$, f) (б) reactions.

Experimental data were analyzed using the missing mass method. Some structure visible on the two-dimensional mass-mass plot (fig. 19) could be interpreted as a manifestation of the three-cluster collinear fission of low excited heavy nuclei. Further study of the problem is evidently needed.

**Complete fusion reactions.**

The electrostatic separator VASSILISSA [59] has been successfully used in FLNR JINR for the experimental study of regularities in the formation and the survival probabilities of excited compound nuclei synthesized in complete fusion reactions with heavy ions. With the use of the separator VASSILISSA, a great bulk of physical investigations on the formation regularities and the survival probabilities of highly excited compound nuclei in the region of $82 \le Z \le 94$ have been carried out. Detailed experimental data for the ER-formation cross sections after proton and alpha particle evaporation from a compound nucleus (the *pxn* and *αxn* evaporation channels) are published in [60].

15 new isotopes of U, Np, Pu and No were synthesized during the experiments at the VASSILISSA separator, and characteristics of its α-decay and SF were studied. Also for a number of known isotopes in the region of Ac – Pa α-decay energy, relative branching ratio and half life data were defined more accurately [61,62]

**Nuclear spectroscopy of heavy nuclei**

The FLNR - IN2P3 (France) collaboration project "Nuclear structure and reaction mechanism studies towards super heavy elements: α-, β-, γ-spectroscopy in very heavy nuclei at Z ≈ 104" is devoted to the focal plane spectroscopy. High intensity and quality beams of the FLNR U-400 cyclotron, availability of unique radioactive targets and the electrostatic separator VASSILISSA make it possible to study heavy (neutron rich) nuclei having formation cross sections of higher than 1 nb.

The detector system consisting of a time-of-flight detector and an array of silicon detectors is installed at the separator focal plane behind the dipole magnet.

Recoil nuclei on passing the time-of-flight detector are implanted into the 16 strip Si stop detector. The active area of the strip detector is 60×60~mm$^2$. Each strip is position sensitive in the vertical direction with a resolution of 0.3 - 0.5 mm.

In the backward direction from the stop detector, 4 electron detectors which cover 30% of the hemisphere are placed. Each electron detector is 50×50 mm$^2$ in size and is divided into 4 strips. The focal plane α- β-detector is surrounded with 7 Ge-γ-detectors (see fig. 20). The Ge detectors together with the BGO anti-compton shields were delivered from the French-UK Loan Pool. The new set-up was given the name of "GABRIELA" – **G**amma **A**lpha **B**eta **R**ecoil **I**nvestigation with the **E**lectromagnetic **A**nalyzer [63].

The energy resolution of 20 keV (FWHM) for α's of the $^{241}$Am ($E_\alpha$=5486 keV) source has been determined for the focal plane stop detector. For the β-detectors the energy resolution of about 8 - 10 keV (FWHM) for 322 keV electrons of the $^{133}$Ba source was measured. The Ge detectors had the resolution of about 2.5 keV for the 1408 keV line of the $^{152}$Eu γ-source [64].

As the illustration of the features of the GABRIELA+VASSILISSA set-up we present here the results of investigation of the odd isotopes $^{253,255}$No produced in the reactions $^{48}$Ca + $^{20}$[illegible] have been studied [65].

**Figure 20**. Detector array at the focal plane of VASSILISSA

In the case of the $^{253-255}$No evaporation residues, their implantation in the stop detector is followed mainly by α-decay. In prompt coincidence with the characteristic α-emission, γ-quanta as well as conversion electrons were detected by GABRIELA.

The spectrum of γ-rays observed in coincidence with the $^{253}$No α-group is shown in fig. 21. It reveals the presence of three main γ-transitions at 150, 221 and 279 keV. The corresponding conversion electron spectrum in fig. 21 shows clearly K- and L-conversion lines of the 279 keV transitions as well as L-conversion lines of the 221 keV transition. The K-line of this transition is masked by a large structure at 50-70 keV. There are possible signs of L-conversion of the 150 keV and weak 130 keV γ-lines (visible to the left of the last Fm K-X-ray group in fig. 21).



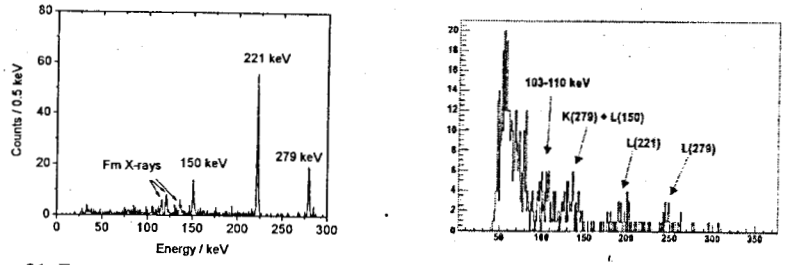


**Figure 21**. Energy spectrum of γ°-rays (left panel) of conversion electrons (in keV, right panel) and de-exciting levels in $^{249}$Fm.

For $^{255}$No, it was observed that many α-decays are followed by delayed γ°- and β-emission. The delayed peak in correlates with the $^{255}$No α-group and indicates the presence of an isomeric state in $^{251}$Fm.. The estimated half life ≈ 30 μs. From the delayed γ- and β- energy spectra, it was found that this isomeric level deexcites mainly by the emission of a highly converted M2 198 keV transition, which explains the observed lifetime.

During past years in 5 campaigns decay properties of 14 heavy isotopes: $^{216,217}$Th, $^{217}$Pa, $^{218,220,221}$U, $^{224,225}$Np, $^{249,251}$Fm, $^{251}$Md, $^{253,255}$No, $^{255}$Lr were investigated using the GABRIELA+VASSILISSA set-up. Detailed experimental data are published in [66-68]

## Theoretical and computational studies

*Reactions with light exotic nuclei.*

A low-energy two-neutron transfer reaction with the Borromean nucleus $^6$He was shown to be an effective instrument for studying both the structure of such nuclei and the dynamics of nuclear reactions with their participation. A four-body model was developed for the first time to describe two-nucleon transfer processes within the distorted-wave Born approximation.

Within a consistent theoretical model it was clearly shown for the first time that the neutron transfer channels with positive Q-values really enhance the fusion cross section at sub-barrier energies [69]. A new process of "sequential fusion" with intermediate neutron transfer to the states with Q>0 was proposed which plays a role of "energy lift" for the two interacting nuclei. The effect was found to be very large especially for fusion of weakly bound nuclei. Within this mechanism a new experiment was proposed for measuring and comparing the evaporation residue cross sections in the $^6$He+$^{206}$Pb and $^4$He+$^{208}$Pb reactions leading to the same compound nucleus. The yield of polonium isotopes at the same energy of 5 MeV below the barrier was predicted to be three orders of magnitude larger for the first reaction as compared to the second one (fig. 22). This experiment has been performed later [70] and the obtained results fully confirmed our predictions. Near-barrier fusion of neutron-rich nuclei was studied also within the time-dependent

three-body Schrödinger equation [71]. It was confirmed that the possibility of neutron transfer with positive Q values considerably increases the barrier penetrability. A huge enhancement of deep sub-barrier fusion probability was found for light neutron-rich weakly bound nuclei. This finding is quite important for understanding of astrophysical primordial and supernova nucleosynthesis.

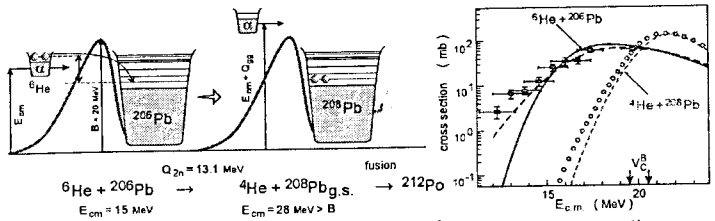


**Figure 22.** Sequential mechanism of sub-barrier fusion of $^{6}$He and the corresponding cross section.

*Synthesis of superheavy nuclei.*

A new mechanism of the fusion-fission process for a heavy nuclear system was proposed, which takes place in a multi-dimensional configurational space describing evolution of nucleon collectivization of two interacting nuclei [72]. These nuclei, surrounded by a certain number of common nucleons dA (shared between the two cores), gradually lose (or acquire) their individualities with increasing (or decreasing) the number of collectivized nucleons dA. For the first time a common driving potential was derived, which allows the calculation of both the probability of the compound nucleus formation and the mass distribution of fission fragments in heavy ion fusion reactions.

Successful theoretical analysis of available experimental data on the "cold" and "hot" fusion-fission reactions was performed within the developed model. The cross sections of superheavy element production with Z = 112–118 in 1n–5n evaporation channels of the $^{48}$Ca induced fusion reactions were predicted [73] and energy positions of maxima of the excitation functions were recommended for subsequent experiments. These predictions have been fully confirmed in the experiments on synthesis of superheavy elements (fig. 23).

Several other reactions leading to the formation of new superheavy nuclei and isotopes including fusion of fission fragments, transfer reactions, and reactions with radioactive ion beams were analyzed along with their abilities and limitations [74]. It was shown that, if the possibility of increasing the beam intensity and the detection efficiency (by a total of one order of magnitude) is found, then several isotopes of new elements with Z = 120–124 could be synthesized in fusion reactions of titanium, chromium, and iron beams with actinide targets.

The use of light- and medium-mass neutron-rich radioactive beams may help us fill the gap between the superheavy nuclei produced in the hot fusion reactions and the continent of known nuclei. In these reactions, we may really approach the "island of stability." Such a possibility is also provided by the multi-



nucleon transfer processes in low-energy damped collisions of heavy actinide nuclei. The production of superheavy elements in fusion reactions with accelerated fission fragments was found less encouraging.

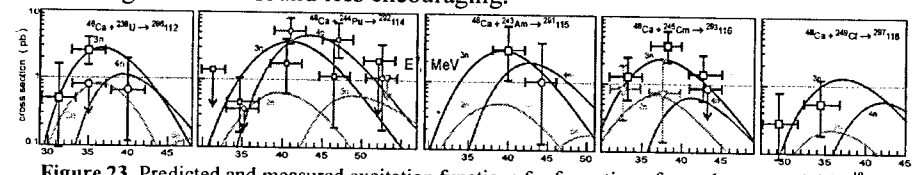


**Figure 23.** Predicted and measured excitation functions for formation of superheavy nuclei in $^{48}$Ca induced fusion reactions.

*Multi-nucleon transfer reactions.*

A new approach based on multi-dimensional Langevin equations was developed for a unified description of strongly coupled deep inelastic scattering, fusion, fission and quasi-fission processes of heavy-ion collisions [75]. The most important degrees of freedom of the nuclear system, a unified time-dependent driving potential [77], and a unified set of dynamic equations of motion are used in this approach.

This makes it possible to perform a full (continuous) time analysis of the evolution of heavy nuclear systems, starting from the approaching stage, moving up to the formation of the compound nucleus and eventually emerging into two final fragments. The calculated mass, charge, energy and angular distributions of the reaction products agree well with the corresponding experimental data on deep inelastic scattering and quasi-fission.

Within the developed model for a unified description of strongly coupled deep inelastic scattering and fusion-fission processes, collisions of very heavy nuclei ($^{238}$U+$^{238}$U, $^{232}$Th+$^{250}$Cf and $^{238}$U+$^{248}$Cm) were investigated as an alternative way for the production of superheavy elements with increasing neutron number [77,78]. It was shown that the shell effects on the multidimensional potential energy surface play an important role in these reactions [79], and an enhanced yield of nuclides far from the projectile and target masses was found in multi-nucleon transfer reactions due to these effects. As a result, the production of surviving superheavy long-lived neutron-rich nuclei is quite possible in low-energy collisions of transactinide nuclei (fig. 24). In many events the lifetime of the composite giant system consisting of two touching nuclei turns out to be rather long (~$10^{-20}$ s), sufficient for observing line structure in spontaneous positron emission from super-strong electric fields, a fundamental QED process not yet confirmed experimentally.

A new way was found to discover and examine unknown neutron-rich heavy nuclei at the "north-east" part of the nuclear map [80,81]. This "blank spot" of the nuclear map can be reached neither in fusion–fission reactions nor in fragmentation processes widely used nowadays for the production of new nuclei. The present limits of the upper part of the nuclear map are very close to stability while the unexplored area of heavy neutron-rich nuclides along the neutron closed shell N =

126 (to the east of the stability line) is extremely important for nuclear astrophysics investigations and, in particular, for the understanding of the r-process of astrophysical nucleogenesis. The estimated yields of neutron-rich nuclei are found to be rather high in such reactions and several tens of new nuclides can be produced, for example, in the near-barrier collision of $^{136}$Xe with $^{208}$Pb. This finding may spur new studies at heavy-ion facilities and should have significant impact on future experiments in nuclear physics.

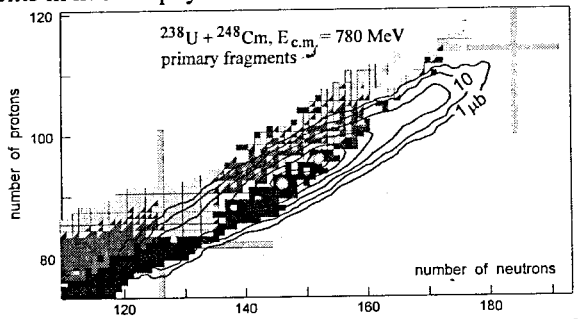


**Figure 24.** Yield of primary neutron-rich heavy fragments produced in collisions of $^{238}$U with $^{248}$Cm at 800 MeV center-of-mass energy (landscape of cross section in logarithmic scale).

*Knowledge base on low-energy nuclear physics.*

The knowledge base on low energy nuclear physics, "Nuclear Reactions Video", allocated at the Web-site http://nrv.jinr.ru/nrv is developed during last several years [82]. The nuclear physics knowledge base solves the two following problems. (1) Fast and visual getting of experimental data on nuclear structure and cross sections of nuclear reactions, a possibility for processing these data, their comparison and plotting the studied regularities and systematizations. (2) Analysis of experimental data and modeling the processes of nuclear dynamics within the foolproof codes based on the well-established physical approaches just in a window of the Web-browser. A set of coupled with each other algorithms of nuclear dynamics, experimental data bases on nuclear structure and nuclear reactions, and a system of special Web codes for analysis, management, representation and handling of user's queries and obtained results of calculations form altogether what is usually called "knowledge base". All recourses of the knowledge base are free and available for any remote user via the Internet by using a standard Web-browser. The knowledge base includes now the following components: (i) Nuclear Map with full experimental information on each nuclide, (ii) experimental data-bases on elastic scattering, complete fusion and evaporation residue Cross Sections, (iii) Optical Model of elastic scattering, (iv) DWBA code for inelastic scattering, (v) Coupled Channel and empirical models of heavy-ion Fusion, (vi) nuclear reaction Kinematics, (vii) nuclear Shell Model, (viii) codes for calculation of Decay Properties of excited nuclei. For the moment this nuclear physics knowledge base is a unique Web-resource of such kind.



## DEVELOPMENT OF FLNR CYCLOTRONS FOR PRODUCING INTENSE BEAMS OF ACCELERATED IONS OF STABLE AND RADIOACTIVE ISOTOPES

Leader: G.G. Gulbekian

## DEVELOPMENT AND CONSTRUCTION OF ACCELERATOR COMPLEX FOR PRODUCING RADIOACTIVE ION BEAMS

Leader: B.N. Gikal, scientific leader: Yu.Ts. Oganessian

Reliable performance of the FLNR accelerators opened wide possibilities for performing new experiments in the low and medium energy range and developing accelerator technology.

The FLNR cyclotron complex is intended for production of intense beams of stable and radioactive ions for studies of exotic nuclei near and beyond the drip-lines.

At present time four heavy ion cyclotrons: U400, U400M, U200, IC100 and electron accelerator – microtron MT25 are under operation in FLNR JINR FLNR. Total operation time is about 11,000 hours per year. For producing of radioactive ion beams like $^{6}$He, $^{8}$He etc. the U400M cyclotron serves as driving- and U400 as postaccelerator. Fission fragments are produced by the use of the electron accelerator MT-25 (DRIBs-II). The layout of the FLNR accelerator complex is presented on fig. 25.

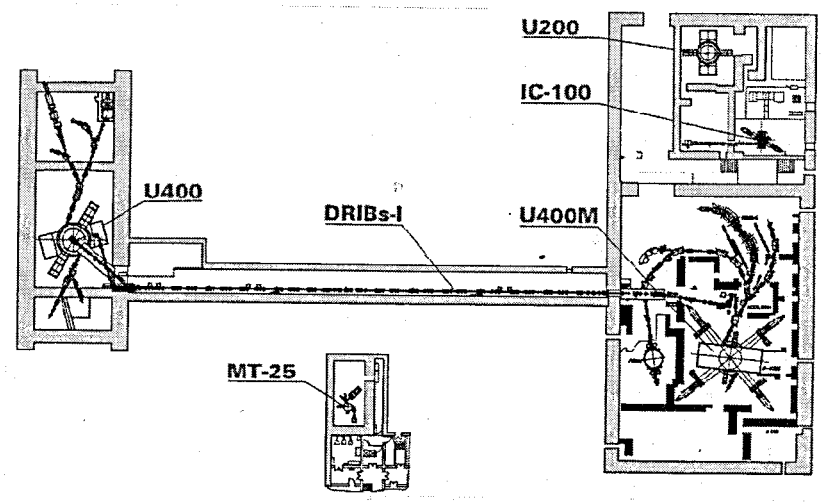


**Figure 25.** Layout of the FLNR JINR accelerator complex

The principal points of the scientific program within the accelerator topics are:

- Development of the FLNR cyclotron complex U400-U400M for producing intense beams of accelerated ions with energies up to 100 MeV/nucleon.
- Upgrade of the U400M cyclotron for the realization of the low-energy mode (6-15 MeV/nucleon).
- Upgrade of the U400 cyclotron to improve the beam quality and reduce power consumption.
- Producing of beams of exotic light neutron-deficient and neutron-rich nuclei in reactions with light ions.
- Producing of uranium photofission fragments.
- Development of ion sources and charge breeders.
- Isotope separation.
- Acceleration of radioactive ions.
- Design of beam diagnostic and transportation systems.

## U400 Cyclotron

The main trend of the cyclotron development is generation of intense beams of medium mass ions, mainly $^{48}Ca$ for experiments research on the synthesis and investigation of properties of new elements, radiochemical experiments, and nuclear spectroscopy. In 2003 – 2009 the total operation time for the cyclotron made 41,000 hours (including tandem operation with U440M for producing of $^{6}He^{2+}$ accelerated ions). About 66% of the total time was used for acceleration of $^{48}Ca^{5+}$ ions for synthesis and investigation of superheavy elements.

The essential modernization of the U400 axial injection included sharp shortening of the horizontal part of the injection canal. To increase the acceleration efficiency, a combination of line and sine bunchers was used. The modernization gave the possibility of increasing the $_{48}Ca^{+5}$ current into the injection line from 40÷60 to 80÷100 μA. Correspondingly, the average output $_{48}Ca^{+18}$ ion current was increased from 20 to 35 μA.

*Reconstruction of the U400 cyclotron → U400R (project).*

The modernization of U400 was proposed for the improvement of the cyclotron parameters. The cyclotron parameters before (U400) and after (U400R) the modernization are shown in Table 1. The aims of the modernization are:

- Decreasing the magnetic field level at the cyclotron center from 1.93÷2.1 T to 0.8÷1.8 T which allows us to decrease the electrical power of the U400R main coil power supply by four times.
- Providing the fluent ion energy variation at the factor of 5 for every mass to charge ratio A/Z at an accuracy of $\Delta E/E=5\cdot10^{-3}$;
- Increasing the beam intensity of accelerated ions by the factor of 3.



Table 1

| Parameters | U400 | U400R |
|---|---|---|
| Electrical power of magnet power supply system | 850 kW | 200 kW |
| The magnetic field level in the magnet center | 1.93÷2.1 T | 0.8÷1.8 T |
| The A/Z range | 5÷12 | 4÷12 |
| The frequency range | 5.42÷12.2 MHz | 5.42÷12.2 MHz |
| The ultimate extraction radius | 1.72 m | 1.8 m |
| K- factor | 305÷625 | 100÷506 |
| Vacuum level | $(1\div5)\cdot10^{-7}$ Top | $(1\div2)\cdot10^{-7}$ Top |
| Ion extraction method | Stripping foil | Stripping foil & Deflector |
| Number of directions for beam extraction | 2 | 2 |

The possibility of increasing the injection voltage from 13÷20 kV to 40÷50 kV is under study. As we estimated, the reconstruction can provide increasing the U400R accelerating efficiency by 1.5÷2 times, it is particularly important for $_{48}Ca$ ions.

The RF system of U400R will consist of two RF generators that will excite two separated RF dee resonators. The RF resonators will be made from iron with copper coating to decrease the outgasing rate from the vacuum surface.

## U400M Cyclotron

In 2003 – 2009 the total operation time for the cyclotron made 22,000 hours (including tandem operation with U440 for producing of $^{6}He^{2+}$ accelerated ions).

At the present time the cyclotron ensures two acceleration modes:

- acceleration of high-energy ion beams up to 100 MeV/nucleon.
- acceleration of low-energy ion beams (the mode providing the beam energy of 4.5-9 MeV/nucleon was implemented in 2008).

As a result low-energy ion beams accelerated at U400M can be used both for production of light radioactive beams and for the studies of superheavy elements at the mass-spectrometer MASHA recently installed at the cyclotron.

Two sources of ions were installed at the U400M cyclotron: an ECR - for the production of heavy ions, and a high-frequency source of ions, which is used for the generation of tritium ion beam. The tritium ion beam was required for the study of $^{4}H$ and $^{5}H$ resonance states in the neutron transfer reactions $t+t\rightarrow{}^{5}H+p$ and $t+t\rightarrow{}^{4}H+d$.

*The channel of low-energy ion beams*

Implementation of low-energy acceleration mode was mainly connected with the program of reconstruction of U400. During this period the research program on

heavy elements should be continued. Thus the possibility of acceleration of medium mass ions like $^{48}Ca$, $^{50}Ti$, $^{54}Cr$, $^{58}Fe$, $^{64}Ni$ must be provided. For this purpose the beam axial injection system and the cyclotron center structure have been reconstructed, and a new system of beam extraction and a new channel (fig. 26) have been created. The project was implemented in 2008, and all systems were tested with accelerated Ar beam.

At the low-energy channel the mass-spectrometer MASHA has been assembled and research equipment for the study of chemical properties of superheavy elements is under assembling. The first experiments are planned in spring 2010.

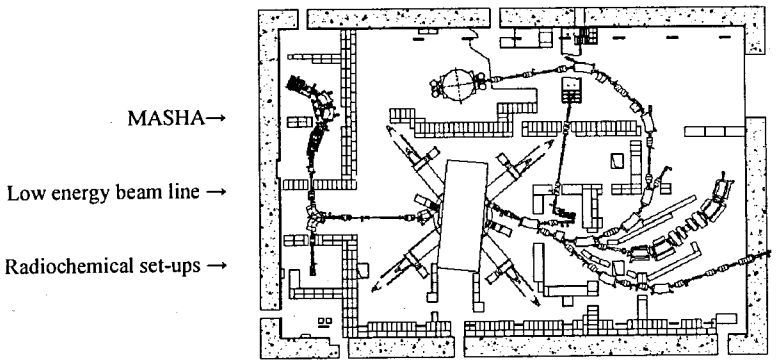


**Figure 26.** Lay-out of the low–energy channel of the U-400M cyclotron

*Tritium acceleration*

At the U400M cyclotron the tritium ions should be accelerated as molecular ions $(DT)^+$ from the point of view beam extraction by stripping. The required beam intensity at the liquid tritium target was about $10^8$ pps. Taking into account the beam losses on transport and monochromatisation, the intensity of the accelerated beam should be about 10 nA ($6 \cdot 10^{10}$ pps).

The main requirements to the ion source were: minimal consumption of radioactive tritium; high output of molecular ions; long life time.

A RF ion source was chosen for the production of molecular ions. During the operation at the test bench the ion source was optimized for the production of $H_2^+$ ions.

For feeding the tritium atoms into the ion source a special gas feed system was developed at RFNC – VNIIEPh (Sarov, Russia) which provides fine regulation of the gas flow and safe handling with tritium.

The hydrogen isotopes, including a deuterium-tritium mixture, are chemically kept on $^{238}U$. After heating the uranium, the hydrogen isotopes flow into the buffer volumes. From the buffer volumes gases are fed into the ion source due to diffusion through the walls of a heated nickel capillary. Special attention was paid to the design of the vacuum system to provide its environmentally safe operation. A beam



of 58-MeV tritons was produced at the U-400M cyclotron and delivered to the tritium target of the ACCULINNA separator.

**The cyclotrons U400 and U400M operating in the DRIBs-I mode**

In this mode of operation the U400M cyclotron serves as driver accelerator of $^7Li$, $^{11}B$, $^{13}C$, $^{15}N$, $^{18}O$ ions with energies of 35 -55 MeV/nucleon providing good possibilities for generation secondary beams of $^6He$, $^{15}B$, $^9Li$, $^{11}Li$, $^{12}Be$, $^{14}Be$, $^8He$.

For producing these beams and their transportation to the postaccelerator U400 a special channel equipped with a target chamber, catcher, ion source for radioactive gas ionization and analyzing magnet were created.

The length of the beam line connecting two cyclotrons makes 120 m. In order to prevent beam losses the pressure of about $10^{-5}$ Pa is maintained in the transportation line.

Table 2 shows the increase of $^6He$ radioactive beam intensity in time resulted from complex continuous improvements.

**Table 2.**

| Year of session | Intensity of $^7Li$ primary beam | Intensity of $^6He$ accelerated beam |
|---|---|---|
| 2004 | 1 pμA | $3\ 10^6$ pps |
| 2006 | 2 pμA | $2\ 10^7$ pps |
| 2008 | 3 pμA | $5\ 10^7$ pps |

The annual operating time of the DRIBs facility amounts to 1-2 months.

**U200 Cyclotron**

The U200 cyclotron has been in operation for more than 40 years. At present the accelerator is used mainly to produce isotopes for use in physical and radiochemical experiments. The annual operating time of the cyclotron amounts to 500-700 hours in the mode of $^4He^{1+}$ acceleration to 36 MeV. A PIG-type internal source is used on the cyclotron. Under development is the project of the beam external injection from an ECR-source which will in general increase the reliability of the accelerator operation.

**IC-100 Cyclic Implanter**

The cyclotron was designed to accelerate ions from carbon ($^{12}C^{+2}$) to argon ($^{40}Ar^{+7}$) with a fixed energy of about 1.2 MeV/nucleon. A PIG-type ion source fully determining the accelerated ion mass limits was used on the accelerator.

In 2003-2005 the IC-100 was modernized. The accelerator was equipped with a system of the beam external axial injection and a superconductive ECR ion source, which allowed generation intensive beams of highly charged ions of xenon, iodine,

krypton, argon and other heavy elements. The intensity of the accelerated and extracted beams on the cyclotron is shown in Table 3.

**Table 3.**

| Ion | Extracted beam |
|---|---|
| $^{22}Ne^{+4}$ | 0.7 μA |
| $^{40}Ar^{+7}$ | 2.5 μA |
| $^{56}Fe^{+10}$ | 0.5 μA |
| $^{86}Kr^{+15}$ | 3.5 μA |
| $^{127}I^{+22}$ | 0.25 μA |
| $^{132}Xe^{+23}$ | 3.7 μA |
| $^{132}Xe^{+24}$ | 0.6 μA |
| $^{182}W^{+32}$ | 0.015 μA |
| $^{184}W^{+31}$ | 0.035 μA |
| $^{184}W^{+32}$ | 0.017 μA |

The IC-100 is equipped with a special beam transportation channel for the polymer film irradiation providing homogeneous ion distribution ion on the target through the area of 600×200 mm$^2$. The lay-out of the IC-100 implantor is shown on the fig. 27.

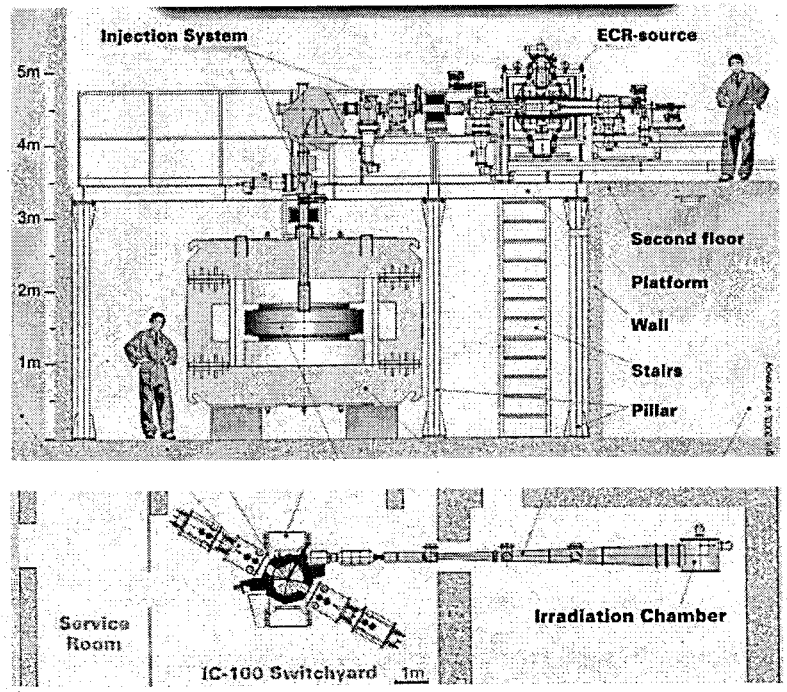


**Figure 27.** Lay-out of the complex for applied research based on the IC-100 cyclic implanter



## Development of ECR-type ion sources

The development of ion sources based on plasma electron heating at the frequency of an electron cyclotron resonance (ECR) is connected with modernization of the Laboratory's accelerator complex - U400, U400M and IC-100 cyclotrons, for producing of intense beams of rare stable isotopes with minimal material consumption and for the generation of secondary radioactive ion beams.

For the last 15 years different types of ERC-sources of the DECRIS family (Dubna Electron Cyclotron Resonance Ion Source) have been developed in the Laboratory.

A superconductive magnetic system is used in the new generation of ion sources (DECRIS-SC) for axial magnetic field formation (maximum distribution of up to 2 T and 3 T). A Gifford McMahon cryo-cooler is used for winding cooling. The magnetic system enables plasma heating at a frequency of 14-28 GHz.

At present, a project of an ECR-source with both axial and radial magnetic fields formation through superconductive winding is being developed.

Sources operating at a frequency of 2.45 GHz have been developed for generation beams of single-charge stable and radioactive ions. The magnetic system of sources consists of rings of permanent (NdFeB) magnets. The sources allow generation beams of single-charge gas ions with an efficiency of ~80 % for Kr and Xe, and ~15% for He. These sources are used in DRIBs-I complex for $^{6}He^{+}$ and $^{8}He^{+}$ ion generation and on MASHA set-up.

## Development and creation of accelerators for other scientific centers

### *DC-72 Cyclotron*

The DC-72 cyclotron has been developed as the basic accelerator facility of the Cyclotron Laboratory (CyLab), Bratislava, Slovakia. The priority fields of using the ion beams of the DC-72 cyclotron include:

- Production of radiopharmaceuticals for diagnostics on the basis of $^{123}I$ and a $^{81}Rb/^{81m}Kr$ generator.
- Neutron capture therapy.
- Fast neutron radiotherapy.
- Eye proton therapy.
- Production of $^{201}Tl$, $^{111}Iu$, $^{67}Ga$ radio-nucleons.
- Fundamental research using reaction products separator.
- Neutron studies and neutron metrology.
- Applied research.

The cyclotron is designed for acceleration of a wide range of ions from protons to heavy ions. Table 4 shows the parameters of accelerated ion beams on the DC-72 cyclotron.

**Table 4.** Beams of accelerated ions on the DC-72 cyclotron.

| Accelerated ion | A/Z | Energy (MeV/nucleon) | Maximum intensity of extracted beams | |
|---|---|---|---|---|
| | | | (eμA) | (pps) |
| $H^-$ | 1 | 72-36 | 50 | $3\cdot10^{14}$ |
| $D^-$ | 2 | 30-15 | 50 | $3\cdot10^{14}$ |
| $^4He^{1+}$ | 4 | 8.6-4.3 | 50 | $1,5\cdot10^{14}$ |
| $^7Li^{1+}$ | 7 | 2.8-1.4 | 3 | $6\cdot10^{12}$ |
| $^{12}C^{3+}$ | 4 | 8.6-4.3 | 20 | $2\cdot10^{13}$ |
| $^{14}N^{3+}$ | 4.7 | 6.2-3.1 | 20 | $1.7\cdot10^{13}$ |
| $^{16}O^{4+}$ | 4 | 8.6-4.3 | 20 | $1.5\cdot10^{13}$ |
| $^{20}Ne^{5+}$ | 4 | 8.6-4.3 | 20 | $1.2\cdot10^{13}$ |
| $^{40}Ar^{8+}$ | 5 | 5.6-2.8 | 10 | $3\cdot10^{12}$ |
| $^{84}Kr^{12+}$ | 7 | 2.8-1.4 | 3 | $7\cdot10^{11}$ |
| $^{129}Xe^{18+}$ | 7.17 | 2.7-1.3 | 1 | $1.6\cdot10^{11}$ |

At present, the cyclotron equipment has been produced in full, has passed full testing at the FLNR and is ready for shipment to Slovakia.

### *DC-60 Cyclotron*

In the Flerov Laboratory of Nuclear Reaction of the JINR, in cooperation with the Institute of Nuclear Physics of the NAS, Kazakhstan, a specialized complex has been created on the basis of the DC-60 cyclotron for the Multidisciplinary Scientific and Research Center (Astana, Kazakhstan). The DC-60 cyclotron is designed for generation of intensive beams of heavy ions from lithium to xenon with energy of 0.35-1.77 MeV/nucleon. On the accelerator there has also been created a channel for low-energy (10-25 keV charge) ion beams obtained from an external ECR-ion source. Table 5 presents the main parameters of the DC-60 cyclotron.

**Table 5.**

| | |
|---|---|
| **Accelerated ions:** | |
| ion mass to charge ratio | 6–12 |
| ion energy, MeV/nucleon | 0.35 –1.77 |
| **Magnetic system:** | |
| magnet length / width / height, mm | 4000 / 1700 / 2300 |
| pole diameter, mm | 1620 |
| magnet mass, ton. | 103.5 |
| magnetic field, T | 1.25 –1.65 |
| Main winding supply power, kW | 45 |
| **High-frequency acceleration system:** | |
| Resonator frequency, MHz | 11–17.4 |
| Dee nominal voltage, kV | 50 |
| Generator power, kW | 20 |
| **ECR-source:** | |
| RF frequency, GHz | 14.3 |
| extraction voltage, kV | 10–25 |
| **Extraction system:** | |
| electrostatic deflector voltage, kV (max) | 60 |



The Center's scientific program is focused mainly on the studies in the solid state physics, nanotechnologies and material surface modification. The cyclotron has three channels for accelerated ion beams. One of the channels is specialized for track membrane production.

The cyclotron center creation started in the beginning of 2004, and at the end of 2006 the accelerator complex was put into operation, the first accelerated beams were obtained and the first experiments performed.

The general view of the DC-60 cyclotron and of the experimental hall is presented on fig.28.

**Figure 28.** General view of the DC-60 cyclotron and of the experimental hall

## Future Development Of The Flerov Laboratory Accelerator Complex (Project DRIBs-III)

The basic role in realization of the plan of researches of the Flerov Laboratory of Nuclear Reactions is associated with creation of accelerator complex DRIBs-III.

The purpose of the project is expansion of a set of accelerated ions, both of stable, and radioactive isotopes, essential increase of intensity and quality of beams.

Realization of project DRIBs-III provides:

- completion of modernization of cyclotrons U400 and U400M,
- creation of a new experimental hall,
- creation of new generation experimental set-ups,
- creation of the high-intensity universal accelerator of heavy ions.

Realization of the Project DRIBs-III in the whole will not only increase by an order of magnitude the efficiency of experiments in the field of SHE synthesis, but will also allow substantially widen the spectrum of researches in the field of heavy and light exotic nuclei.

## REFERENCES


[1] Yu.Ts. Oganessian. *J. Phys. G: Nucl. Part. Phys.* **34** (2007) R165-R242.
[2] Yu.Ts. Oganessian, Yu.V. Lobanov, A.G. Popeko et al., *JINR LNR Scientific Report* 1989–1990, *Heavy Ion Physics*, Dubna, 1991, 158.
[3] Yu. Ts. Oganessian, V. K. Utyonkov, Yu. V. Lobanov et al., *Phys. Rev.* C **64** (2001) 064309.
[4] Yu.Ts. Oganessian, V.K. Utyonkov, Yu.V. Lobanov et al., *Phys. Rev.* C **70**, 064609 (2004);.
[5] Yu.Ts. Oganessian, V.K. Utyonkov, Yu.V. Lobanov et al., *Phys. Rev.* C **62**, 041604 (R), 2000.
[6] Yu.Ts. Oganessian, V.K. Utyonkov, Yu.V. Lobanov et al., *Phys. Rev.* C **69**, 054607 (2004).
[7] Yu.Ts. Oganessian, V.K. Utyonkov, Yu.V. Lobanov et al., *Phys. Rev.* C **69**, 021601(R) (2004).
[8] Yu.Ts. Oganessian, V.K. Utyonkov, S.N. Dmitriev et al., *Phys. Rev.* C **72**, 034611 (2005).
[9] S.N. Dmitriev, Yu.Ts. Oganessyan, V.K. Utyonkov et al., *Mendeleev Commun.* 1 (2005).
[10] R. Dressler, R. Eichler, D. et al., *Phys. Rev.* C **79**, 054605 (2009)
[11] N.J. Stoyer et al 2006 Proc. 9th Int. Conf. Nucl. – Nucl. Collisions (Rio de Janeiro, Brazil, 28 Aug. – 1 Sep.
[12] Yu.Ts. Oganessian, V.K. Utyonkov, Yu.V. Lobanov et al., *Phys. Rev.* C 63, 011301(R) (2001).
[13] Yu. Ts. Oganessian, V. K. Utyonkov, Yu. V. Lobanov et al., *JINR Communication* D7-2002-287 (2002).
[14] Yu.Ts. Oganessian, *Phys. Scr.* **125** (2006) 57
[15] Yu. Ts. Oganessian, V. K. Utyonkov et al. *Phys. Rev.* C **76**, 011601(R) (2007)
[16] M. Gupta, T. W. Burrows, *Nucl. Data Sheets* **106** (2005) 251.
[17] D.S. Hoffman, *Nucl.Phys.*A **502**, 21c , 1989.
[18] A. Baran, Z. Łojewski, K. Sieja, *Int. J. Mod. Phys.* E **15** (2006) 452.
[19] A.B. Yakushev et al., 2001 *Radiochim. Acta* **89** 743.
[20] R. Eichler et al., *Nature*, **447** (2007), p.72-75.
[21] R. Eichler et al. *Angew. Chem. Int. Ed.* **47(17)**, 3262-3266 (2008).
[22] Ch.E. Düllman et al., *Nucl. Exp. Meth.* A479 (2002) 631.
[23] R.Eichler et al., submitted to *Nature* (2009)
[24] Yu. Ts. Oganessian, V. K. Utyonkov, *Phys. Rev.* C **79**, 024603 (2009)
[25] Yu. Ts. Oganessian, S. N. Dmitriev et al., *Phys. Rev.* C **79**, 024608 (2009)
[26] S.I. Sidorchuk et al., *Phys. Lett.* B594 (2004) 54-60.
[27] M.S. Golovkov et al., *Phys. Lett.* B**588** (2004) 163.
[28] M.S. Golovkov et al., *Phys. Rev. Lett.* **93** (2004) 262501.
[29] M.S. Golovkov et al., *Phys. Rev.* C **72** (2005) 064612.
[30] M.S. Golovkov et al., *Phys. Rev.* C **76** (2007) 021605(R).
[31] M.S. Golovkov et al., *Phys. Lett.* B **672** (2009) 22-29.
[32] Ю.Э. Пенионжкевич и С.М. Лукьянов. *ЭЧАЯ* **37**(2) (2006) 439-492.
[33] Ю.Г. Соболев и др., *Изв. РАН*, сер. физ., **69** (2005) 1605-1609.
[34] Yu.E. Penionzhkevich et al., *Eur. Phys. J.* A **31** (2007) 185-194.
[35] S.M. Lukyanov et al., *Phys. Lett.* B **670** (2009) 321-324.
[36] Yu.E.Penionzhkevich. Phys.Atomic Nuclei 72, 1617 (2009).
[37] A.A. Kulko et al., *J. Phys. G: Nucl. Part. Phys.* **34** (2007) 2297–2306.
[38] Yu.E. Penionzhkevich et al., *J. Phys. G: Nucl. Part. Phys.* **36** (2009) 025104.
[39] Yu.E. Penionzhkevich et al., *Int. J. of Modern Phys.* E **17**(10) (2008) 2349-2353.
[40] Р. Калпакчиева и др., *Яд. Физ.* **70**(4) (2007) 649-655.





[41] N.A. Kondratiev et al., Proc. of the 4th Int. Conf. on Dynamical Aspects of Nuclear Fission (DANF 1998), Oct. 1998, Casta-Papiernichka, Slovac Republic, World Scientific, Singapore (1999) 431.
[42] E.M. Kozulin et al., *Instr. Exp. Techniques*, **51**(10) (2008) 44–58.
[43] A. Bogachev et al., *Eur. Phys. J.* A **34**, 23–28 (2007).
[44] M.G. Itkis et al., *Phys. Rev.* C **67**, 011603 (2003).
[45] I.M.Itkis et al., *Phys. Lett.* B **640**, 23, 2006.
[46] R.N. Sagaidak et al., *Phys. Rev.* C **68**, 014603 (2003).
[47] G.N. Knyazheva et al., Phys. Rev. C **75**, 064602 (2007).
[48] E.V. Prokhorova et al., Nucl. Phys. A **802** (2008) 45-66.
[49] M.G. Itkis et al., Proc. of the Int. Conf. on Fusion Dynamics at the Extremes, Dubna, 2000, World Scientific, Singapore (2001) 93.
[50] M.G. Itkis et al., Proc. of the 2nd Int. Conf. on Fission and Properties of Neutron- Rich Nuclei, St. Andrews, Scotland, June28-July 3, 1999 Eds. J. H. Hamilton et al., World Scientific, Singapore (2000) p.268.
[51] I.M. Itkis et al., Proc. Int. Symp. EXON2004, Peterhof, Russia, 5-12 July 2004, World Scientific, Singapore (2005 ) 317.
[52] M.G. Itkis et al., et al., Proc. of the 5th Int. Conf. on Dynamical Aspects of Nuclear Fission (DANF 2001), Oct. 23-27, 2001, Casta-Papiernichka, Slovac Republic, World Scientific, Singapore., (2003) 1.
[53] M.G. Itkis et al., *Nucl. Phys.* A **734** (2004) 136.
[54] M.G. Itkis et al., *Phys. At. Nucl.*, **66** (2003) 1118.
[55] V.I. Zagrebaev, M . G. Itkis, Yu. Ts. Oganessian, *Phys of At. Nucl.*, **66** (2003) 1033.
[56] M.G. Itkis, Yu. Ts. Oganessian, V. I. Zagrebaev, *Phys. Rev.*, C**65** (2002) 044602.
[57] M.G. Itkis et al., *Nucl. Phys.* A **787** (2007) 150-159.
[58] Yu. Pyatkov et al., Proc. Int. Symp. EXON-2006, Khanty-Mansiysk, 17-22 July 2006, AIP Press, p.144.
[59] O.N. Malyshev et al., *Nucl. Instr. and Meth.* A **516** (2004) 529.
[60] A.V. Yeremin et al., *Phys. At. Nucl.* **66**(6) (2003). 1042-1052.
[61] A.V. Belozerov et al., *Eur. Phys. J.*, A. **16** (2003). 447-456.
[62] A.V. Yeremin, *Phys. Elem. Part. At. Nucl.*, **38** (2007), 939.
[63] A G. Popeko *et al., Phys. of At. Nucl.* **69**, 1183 (2006)
[64] K. Hauschild *et al., Nucl. Instr. & Meth. A* **560**, 388 (2006).
[65] A. Lopez-Martens *et. al., Phys. Rev. C* **74**, 044303 (2006).
[66] A. Lopez-Martens et al., *Eur. Phys. J.* A **32**, 245 - 250 (2007).
[67] A. Lopez-Martens et al., *Eur. Phys. J* A**32** (2007) 245
[68] K. Hauschild et al., *Phys. Rev.* C **78** (2008) 021302
[69] V.I. Zagrebaev, *Phys. Rev.*, **C67** (2003) 061601(R).
[70] Yu. Penionzhkevich et al., *Phys. Rev. Lett.*, **96** (2006) 162701.
[71] V.I. Zagrebaev, V.V. Samarin and Walter Greiner, *Phys. Rev.*, **C75** (2007) 035809.
[72] V.I. Zagrebaev, *Phys. Rev.*, **C64** (2001) 034606.
[73] V.I. Zagrebaev, *Nucl. Phys.*, **A734** (2004) 164.
[74] V.I. Zagrebaev and W. Greiner, *Phys. Rev.*, **C78** (2008) 034610.
[75] V.I Zagrebaev and W. Greiner, *J. Phys. G: Nucl. Part. Phys.*, **31** (2005) 825
[76] V.I. Zagrebaev et al., *Phys. Part. Nucl.*, **38** (2007) 469.
[77] V.I.Zagrebaev et al., *Phys. Rev.*, **C73** (2006) 031602(R)
[78] V.I. Zagrebaev and W. Greiner, *J. Phys. G: Nucl. Part. Phys.*, **34** (2007) 1.
[79] V.I. Zagrebaev and W. Greiner, *J. Phys. G: Nucl. Part. Phys.*, **34** (2007) 2265.
[80] V.I. Zagrebaev and W. Greiner, *Phys. Rev. Lett.*, **101** (2008) 22701.
[81] V.I. Zagrebaev and W. Greiner, *J. Phys. G: Nucl. Part. Phys.*, **35** (2008) 125103.
[82] V.I Zagrebaev et al., *Low energy nuclear knowledge base*, http://nrv.jinr.ru/nrv.